

ゲルマニウム添加シリカガラスにおける
欠陥の構造とその光非線形性発現に果たす役割

課題番号 06452222

平成7年度科学研究費補助金（一般研究B） 研究成果報告書

平成8年 3月

研究代表者 大木 義路

（早稲田大学理工学部教授）

は し が き

本報告書は下記の課題で助成を受けた文部省平成7年度科学研究費補助金（一般研究B）に関わる研究成果をまとめたものである。

研究課題

ゲルマニウム添加シリカガラスにおける欠陥の構造とその光非線形性発現に果たす役割

課題番号 06452222

研究組織

研究代表者： 大木 義路

（早稲田大学理工学部教授）

研究分担者： 浜 義昌

（早稲田大学理工学総合研究センター教授）

研究分担者： 宗田 孝之

（早稲田大学理工学部助教授）

研究経費

平成6年度	5,600千円
平成7年度	1,800千円
計	7,400千円

研究発表

（ア）学会誌

- ・ Makoto Fujimaki, Kwang Soo Seol, and Yoshimichi Ohki, "Excited-state absorption measurement in Ge-doped SiO₂ glass.", Optics Letters, (投稿中)
- ・ Makoto Fujimaki, Kanta Yagi, Yoshimichi Ohki, Hiroyuki Nishikawa, and Koichi Awazu, "Laser-power dependence of absorption changes in Ge-doped SiO₂ glass induced by a KrF excimer laser.", Physical Review B. (1996年4月掲載予定)
- ・ Kwang Soo Seol, Akihito Ieki, Yoshimichi Ohki, Hiroyuki Nishikawa, and Masaharu Tochimori, "Photoluminescence study on defects in buried SiO₂ film formed by implantation of oxygen", Journal of Applied Physics, 79, 412-416, 1996.
- ・ Hiroyuki Nishikawa and Yoshimichi Ohki, "Paramagnetic defect centers induced by excimer lasers, γ rays, and mechanical fracturing in amorphous SiO₂", Defect and Diffusion Forum, 123-124, 123-134, 1995.

(イ) 国際会議発表

- ・ Kwang Soo Seol, Akihito Ieki, Yoshimichi Ohki, Hiroyuki Nishikawa, and Masaharu Tachimori, "Luminescence properties of defects in P⁺- or B⁺-implanted thermally grown silicon dioxide", 1995 International Symposium on Electrical Insulating Materials, Tokyo, Japan (1995年9月18日)
- ・ Makoto Fujimaki, Kanta Yagi, Yoshimichi Ohki, Hiroyuki Nishikawa, Koichi Awazu, Kenichi Muta, and Makie Kato, "Laser-power Dependence of KrF Excimer Laser Induced Absorption in Ge-doped SiO₂ Glass", VIII International Conference on the Physics of Non-crystalline Solids (1995年6月29日)
- ・ Makoto Fujimaki, Yoshimichi, Hiroyuki Nisikawa, Koichi Awazu, and Kenichi Muta, "Optical Absorption and Photoluminescence of Defect in Germanium-doped Silica Glass", Materials Research Society Fall Meeting (1994年11月30日)

(ウ) 国内学会発表

- ・ 藤巻真、薛光洙、大木義路、"Ge ドープ SiO₂ ガラスにおける時間分解励起状態吸収測定"、電気学会全国大会(1996年3月28日)
- ・ 藤巻真、薛光洙、大木義路、"Ge ドープ SiO₂ ガラスにおける励起状態吸収測定"、第43回応用物理学関係連合講演会(1996年3月26日)
- ・ 藤巻真、八木幹太、大木義路、西川宏之、栗津浩一、牟田健一、加藤真基重、"Ge ドープ SiO₂ ガラスにおける KrF エキシマレーザ誘起吸収のフォトブリーチ"、第56回応用物理学会学術講演会(1995年8月27日)
- ・ 八木幹太、藤巻真、大木義路、西川宏之、栗津浩一、牟田健一、加藤真基重、"Ge ドープ SiO₂ ガラスのエキシマレーザ光多量照射による光吸収変化"、第42回応用物理学関係連合講演会(1995年3月28日)
- ・ 藤巻真、八木幹太、大木義路、西川宏之、栗津浩一、牟田健一、加藤真基重、"Ge ドープ SiO₂ ガラスにおける KrF エキシマレーザ誘起光吸収のレーザパワー依存性"、第55回応用物理学会学術講演会(1994年9月21日)
- ・ 藤巻真、八木幹太、大木義路、西川宏之、栗津浩一、牟田健一、加藤真基重、"Ge ドープ SiO₂ ガラスの発光の励起帯の温度依存性"、第55回応用物理学会学術講演会(1994年9月21日)
- ・ 藤巻真、西川宏之、大木義路、"Ge ドープシリカガラスのエキシマレーザ誘起ルミネセンス"、第54回応用物理学会学術講演会(1993年9月27日)

研究成果

(1) 研究の目的

ゲルマニウム (Ge) ドープシリカガラスは光ファイバとして重要であるばかりでなく、近年ではレーザ光を照射することにより、第2次高調波発生 (SHG) といった非線形光学現象や、屈折率変化といった興味深い効果が誘起されることが報告さ

れ注目を集めている。現在までの処、強力レーザー光により Ge ドープシリカガラス中に多数の点欠陥が空間的に規則正しく誘起されることがこれらの現象に対して大きな役割を果たしていると考えられるようになってきた。しかし、欠陥の詳細構造や欠陥が誘起されるメカニズム、欠陥が諸効果に果たす役割については不明な点が多く残されている。そこで本研究において、反磁性欠陥について、可視～真空紫外域での光吸収、ルミネッセンスの時間分解スペクトル、常磁性欠陥について、主として ESR により欠陥構造とその生成機構を明らかにする。ついで、SHG や屈折率変化の誘起強度と各欠陥量、欠陥構造から推定される双極子能率等の対応を求めていくことにより、如何なる欠陥がどのような機構で諸効果を誘起しているのかを明らかにすることを目的とする。本研究により欠陥構造等の解明が進むことは、第一に、光ファイバとして最も多用されている Ge ドープシリカの可視～紫外域光伝送媒体としての利用拡大や長期信頼性などに大きく貢献すると考えられる。第二点として、本研究により、欠陥構造と非線形光学効果誘起現象との関係が明らかになることは、非線形光学素子の開発に寄与することはもちろんであるが、反転対称性を有するガラスにおける非線形光学機構が明らかになることにより、新しい概念にもとづく素子の提案に寄与できると思われる。

(2) 研究成果の概要

1. ゲルマニウム添加シリカガラスの欠陥構造について

1-1 Ge ドープ SiO₂ ガラスは通信用光ファイバの材料としてだけでなく、その光感受性を利用し、内部に構造変化を生じさせることにより、光ファイバ自体に機能性を持たせるファイバ型素子の材料としても注目を集めている。なかでも光ファイバブレッティングは光ファイバ内にブラッグブレッティングを形成し特定の波長のみ反射することのできる光フィルタとして、現在開発が進められている。このブラッグブレッティングは、紫外光照射により生じる構造変化に伴う屈折率の変化を光ファイバ内に格子状に形成することにより作製される。

本研究においては、主として、照射光源として KrF エキシマレーザを用い、高密度のフォトンがガラスに照射されたときの構造変化について、主に光吸収および ESR 等の手法を用い解析を行った。酸素欠乏型の Ge ドープ SiO₂ ガラスには、5eV 付近に非常に大きな吸収帯が見られる。KrF エキシマレーザをサンプルに照射するところの吸収帯が減少し、4.5eV および 5.8eV にピークを持つ吸収帯が誘起される。我々は、これらの吸収帯の誘起は照射光密度と非常に深い関係があることを発見した。これらの吸収変化の飽和値は、照射光強度が大きいほど大きくなり、また高フォトン密度のレーザー光で誘起された吸収は、低フォトン密度のレーザー光によりブリーチされることが分かった。このことから、この光誘起吸収変化は光照射による吸収の誘起過程とブリーチ過程の平衡反応であると考えられる。吸収の誘起過程は、高フォトン密度のレーザー光により効果的に誘起され、誘起吸収のブリーチが低フォトン密度光を照射したときに生じることから、吸収誘起過程はレーザー光照射時の 2

光子過程で生じ、ブリーチは、1光子過程で生じていると考えた。この考えに基づき、測定結果に対し数値解析を行ったところ、良い一致を得ることができた。KrFエキシマレーザ照射時には、常磁性欠陥である germanium electron-trapped center (GEC) が誘起されるが、誘起される GEC 濃度と誘起吸収変化量の間に良い比例関係があり、またこの吸収変化が、酸素欠乏型のサンプルで効果的に生じることから、KrFエキシマレーザ照射時に生じる吸収変化は、酸素欠乏性欠陥がレーザ照射時の2光子過程により電子を放出し、その電子が GEC を形成し、またその逆反応が1光子過程により生じることが明らかになった。

1-2 前節で述べたように、酸素欠乏型の Ge ドープ SiO₂ ガラスは、5eV に吸収帯を持ち、この吸収帯を励起することにより 4.3eV と 3.1eV にピークを持つ発光帯が誘起される。これらの発光帯は、それぞれ酸素欠乏性欠陥の励起一重項状態 (S₁)、励起三重項状態 (T₁) から基底状態 (S₀) への電子遷移により生ずるとされている。S₁-S₀ 遷移は許容遷移であるため 4.3eV 発光の寿命は非常に短い。我々は軌道放射光を用いた単一光子計数法により初めてその時定数を正確に計測し、これが 9ns であることを明らかにした。

一方 3.1eV 発光は T₁-S₀ 遷移が禁制遷移であるため、その時定数は 114 μs と 4.3eV 発光のそれよりは遥かに長い。さらに、S₁ から T₁ への緩和時間も 5.3ns と非常に短いとされているため、高エネルギー光でこの欠陥を励起したときには、欠陥の基底状態から励起された電子の殆どが T₁ に存在するような状況を実現することができる。このように、T₁ 状態に長時間電子が存在していることから、T₁ からさらに上準位への励起が可能ではないかと考えた。すなわち、KrFエキシマレーザを励起光源に用い欠陥の電子を励起した後、100ns~200 μs 後に Xe フラッシュランプを入射し、透過光スペクトルを測定するという一種のポンプ-プローブ法により励起状態吸収の時間分解測定を試みた。その結果、3.1eV 発光と同じ時定数を持って減衰していく 3eV 付近から立ち上がり 4eV 以上にピークを持つ吸収帯が観測された。時定数の一致より、この吸収帯は T₁ 状態からさらに上準位への電子遷移による吸収であるといえる。その上準位が何であるかについては、観測された吸収帯が比較的にブロードであること、準位が S₀ から約 6eV 付近から立ち上がっていること、及び Ge ドープ SiO₂ ガラスのバンドギャップが約 7eV であることから、Ge ドープ SiO₂ ガラス自身の伝導帯であると考えられる。今回 T₁ 状態からの励起が測定できたことは、酸素欠乏性欠陥の光学的特性の理解を深める上でも、また T₁ 状態からの励起により、欠陥のイオン化が基底状態からのイオン化よりも低エネルギーのフォトンで行えるという可能性の追求においても大きな意味を持つ。

2. 純粋シリカガラスの欠陥構造について (シリカガラス薄膜での欠陥について)

Si デバイスにおける高速・高出力デバイスの発展に伴って、寄生容量や側面絶縁などが重要な問題になっている。これらの問題を解決するため、silicon-on-

insulator 構造をもつ基板に対する様々な製造方法が開発されている。その中で、単結晶シリコン中に高エネルギーをもつ酸素イオンを注入しシリコン層の中に埋め込み酸化層を作る方法が最も有効な方法として期待されている。この方法は一般に SIMOX (Separation by implanted oxygen) と呼ばれている。しかしながら、この SIMOX 法で作られた埋め込みシリコン酸化膜を持つデバイスは、通常の熱酸化膜を持つデバイスと比べ、電気伝導度や電荷蓄積の面において、あるいは、欠陥生成の異常増加などの幾つかの問題点が指摘されている。また、これらの問題点に対して、SIMOX 埋め込み酸化膜と通常の熱酸化膜との構造や均一性、あるいは、化学量論比よりのずれ等の相違が主な原因として考えられている。この観点から、SIMOX 埋め込み酸化膜の特性に対する様々な研究が進行中である。

本研究においては、その測定が極めて困難であることから殆ど行われていなかったこれら薄膜シリコン酸化膜からのフォトルミネセンスを検出することにより、SIMOX 埋め込み酸化膜に対する点欠陥の評価を試みた。実験に用いた SIMOX 埋め込み酸化膜は、p 型 (100) Si 基板に酸素を加速電圧 180 keV でドーズ量 $1.7 \times 10^{16} / \text{cm}^2$ まで注入し、その後、Ar+O₂ 雰囲気、1350°C で 6 時間アニールし形成した。フォトルミネセンス (PL) スペクトルは KrF エキシマレーザで励起し、マルチチャンネルディテクタで測定を行った。PLE (photoluminescence excitation) は、軌道放射光を用い測定を行った。その結果として、SIMOX 埋め込み酸化膜から 4.3 eV と 2.7 eV の発光を観測、また、4.3 eV 発光に対して、5.0 eV と 7.4 eV の PLE バンドを確認した。各発光帯に対して、時間分解測定を行った結果、4.3 eV 発光は数 ns の寿命 (5.0 eV フォトン励起の場合： 4.0 ns, 7.4 eV で励起の場合： 2.4 ns) を持ち、2.7 eV 発光帯は 10 ms の発光寿命を持つことが分かった。これらの発光特性はシリカガラスにおける酸素空孔によるそれと完全に一致していることから、この発光が酸素空孔欠陥によるものであることが分かった。また、埋め込み SIMOX 酸化膜の膜厚変化に対する発光強度変化からこの酸素空孔欠陥が膜中にほぼ均一に分布していることが確認され、さらに、各シリコン酸化膜 (イオン注入熱酸化膜、熱酸化膜、SIMOX 埋め込み酸化膜) におけるこれらの発光強度の比較によって、SIMOX 埋め込み酸化膜に酸素空孔欠陥が熱酸化膜より大量に存在していることが確認された。この大量に存在する酸素空孔欠陥が正孔トラップや電子供給源として働き、SIMOX 埋め込み酸化膜の異常特性 (電荷蓄積や電気伝導等の異常増加) の原因となる可能性を世界で初めて指摘した。

主な研究成果

Excited-state absorption measurement in Ge-doped SiO₂ glass

Makoto Fujimaki, Kwang Soo Seol, and Yoshimichi Ohki

*Department of Electrical Engineering , Waseda University, 3-4-1 Okubo,
Shinjuku-ku, Tokyo 169, Japan*

Abstract

Optical absorption change in the microsecond order in oxygen-deficient Ge-doped silica glass was measured as a function of time just after photon irradiation from a KrF excimer laser. The absorption above 3 eV was found to decay with the same time constant as that of the luminescence at 3.1 eV. From this, it is confirmed that the observed absorption change is due to the excitation of electrons from the lowest excited triplet state to an upper state.

Germanium-doped SiO₂ glass is a key component for telecommunication optical fibers. Furthermore, Ge-doped SiO₂ glass, especially its oxygen-deficient type, is attracting much attention as optical fiber gratings. This type of SiO₂ glass has an absorption band at 5 eV. By exciting this absorption band, two photoluminescence (PL) bands appear at 4.3 eV and 3.1 eV. Since the 4.3 eV PL has a short lifetime ($\tau < 10$ ns), it is assigned to electron transition from the lowest excited singlet state (S_1) to the ground state at a germanium oxygen-deficient type center (GODC), while the 3.1 eV PL is assigned to that from the lowest triplet state (T_1) to the ground state because of its long lifetime ($\tau \doteq 114$ μ s).¹⁻³ However, the exact structure of GODC is still debatable, mainly between the neutral oxygen vacancy ($\equiv \text{Ge}-\text{Ge} \equiv$, ‘ \equiv ’ denotes bonds with three separate oxygens) and the germanium lone-pair center ($-\ddot{\text{Ge}}-$, ‘ $\ddot{\cdot}$ ’ denotes lone-pair electrons).^{1,4} One way to find a clue to the elucidation of its structure is to study its excited states. When Ge-doped SiO₂ glass is exposed to intense 5.0 eV photons from a KrF excimer laser, electrons are first excited to S_1 state. However, since the electron lifetime at T_1 state is much longer than that at S_1 state and the transition time from S_1 state to T_1 state is very fast ($\tau = 5.3$ ns), plenty of excited electrons stay at T_1 state.³ Therefore, there is a possibility that the absorption due to electronic excitation to an upper state from T_1 state can be observed.

However, to our knowledge, such an observation has not been reported. This paper presents a result of excited-state absorption measurement in oxygen-deficient Ge-doped SiO₂ glass by a pump-probe method.

Figure 1 shows the measurement system. The samples used are oxygen-deficient type glass of 95SiO₂:5GeO₂ prepared by the vapor-phase axial deposition method. The samples were cut and polished into plates of 0.3 mm thick. A KrF excimer laser (MPB Technologies, PSX-100) was used as the light source for pumping electrons to the excited states. The energy density per pulse and the pulse width of the excimer laser are 1 mJ/cm² and 5 ns, respectively. To observe the transient absorption, a Xe flash lamp was irradiated for some observation time to the sample after a delay of fixed time. The transmission spectrum dispersed by a monochromator (Jobin Yvon, HR320) was observed by a multi-channel detector (Princeton Instruments, IRY700) with an image intensifier. The flash lamp and the detector were operated by a four-channel digital delay/pulse generator (Stanford Research Systems, DG535), which controls the start of measurement so that the incident photon number to the sample from the flash lamp becomes constant as long as the observation time is constant, since the luminosity of the flash lamp varies with time. The absorption from the ground state which had been obtained without the pumping was automatically subtracted from the transmission

spectrum by computer. The PL induced by the irradiation of the KrF excimer laser is observed as a negative absorption change. In this experiment, the observation time or the exposure of the flash lamp is 30 ns and the delay time between the pumping and the start of exposure is changed from 100 ns to 200 μ s. Because of a band-pass filter used to eliminate the scattering light of 5 eV from the pumping laser and the ability of the detector, the measurement was limited in the range of 1.55 to 4 eV.

Figure 2 shows the result. A transient absorption band induced by the irradiation of the excimer laser is seen above about 3.5 eV. The negative peak around 3.1 eV is the simultaneously-induced PL band caused by the electronic transition from T_1 state to the ground state. From this figure, it is observed that the transient absorption band decreases with the same time constant as that of the PL intensity. In other words, this transient absorption occurs only when electrons exist at T_1 state. From this experimental result, it is confirmed that the transient absorption is caused by the electronic transition from T_1 state to an upper state. In order to know the correct position of the absorption edge, the effect of PL must be subtracted. For this purpose, the 3.1 eV PL spectrum as a function of time was obtained without using the flash lamp, and it was subtracted from the corresponding spectrum in Fig. 2. Figure 3 shows the result. It is obvious

that the transient absorption band is very broad, starting around 3 eV with its peak above 4 eV. That is to say, this absorption band lies in the region from 6 to more-than-7 eV from the ground state. Since the energy gap of Ge-doped SiO₂ glass is 7.1 eV⁵, there is a possibility that the upper state is the conduction band.

The present success of the observation of the electronic excitation from T₁ state is important to elucidate the optical property of GODC. Furthermore, it shows the possibility that ionization of GODC is caused by low energy photons by a cumulative two-photon excitation (or up-conversion) through T₁ state.

The authors express their thanks to Dr. K. Muta and M. Kato of Showa Electric Wire and Cable, for providing the samples, and to G. Sarata of Waseda University for his help in doing experiments. Their appreciation is also extended to Dr. H. Nishikawa of Tokyo Metropolitan University and Dr. K. Awazu of Electrotechnical Laboratory for their encouragement. This work was partly supported by a Grant-in-Aid from the Ministry of Education of Japan.

that the transient absorption band is very broad, starting around 3 eV with its peak above 4 eV. That is to say, this absorption band lies in the region from 6 to more-than-7 eV from the ground state. Since the energy gap of Ge-doped SiO₂ glass is 7.1 eV⁵, there is a possibility that the upper state is the conduction band.

The present success of the observation of the electronic excitation from T₁ state is important to elucidate the optical property of GODC. Furthermore, it shows the possibility that ionization of GODC is caused by low energy photons by a cumulative two-photon excitation (or up-conversion) through T₁ state.

The authors express their thanks to Dr. K. Muta and M. Kato of Showa Electric Wire and Cable, for providing the samples, and to G. Sarata of Waseda University for his help in doing experiments. Their appreciation is also extended to Dr. H. Nishikawa of Tokyo Metropolitan University and Dr. K. Awazu of Electrotechnical Laboratory for their encouragement. This work was partly supported by a Grant-in-Aid from the Ministry of Education of Japan.

¹M. J. Yuen, Appl. Opt. **21**, 136 (1982).

²L. Skuja, J. Non-Cryst. Solids **149**, 77 (1992).

³V. N. Bagratashvili, V. K. Popov, S. I. Tsykina, P. V. Chernov, and A. O. Rybaltovskii, Opt. Lett. **20**, 1619 (1995).

⁴M. Kohketsu, K. Awazu, H. Kawazoe, and M. Yamane, Jpn. J. Appl. Phys. **28**, 622 (1989).

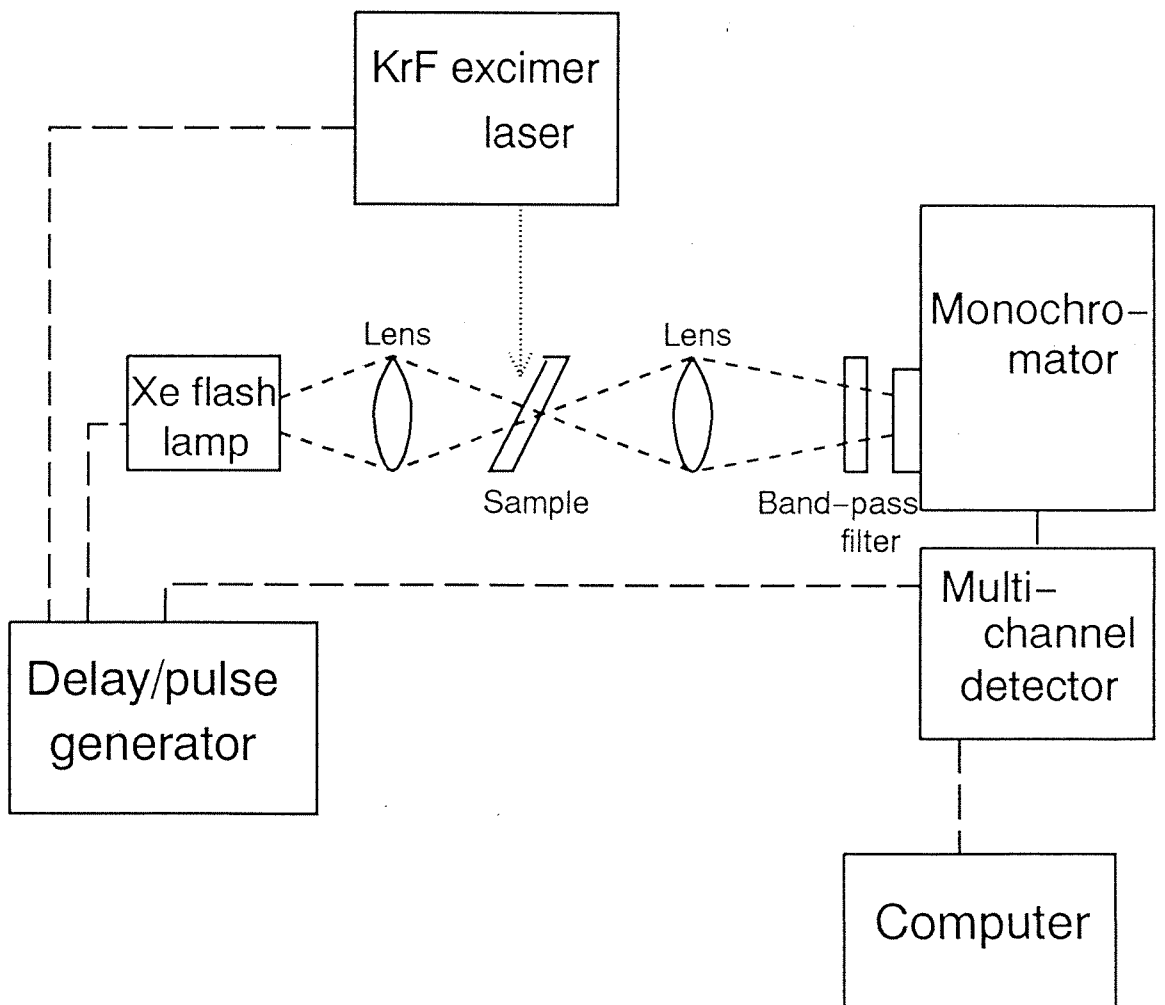
⁵J. Nishii, N. Kitamura, H. Yamanaka, H. Hosono, and H. Kawazoe, Opt. Lett. **20**, 1184 (1995).

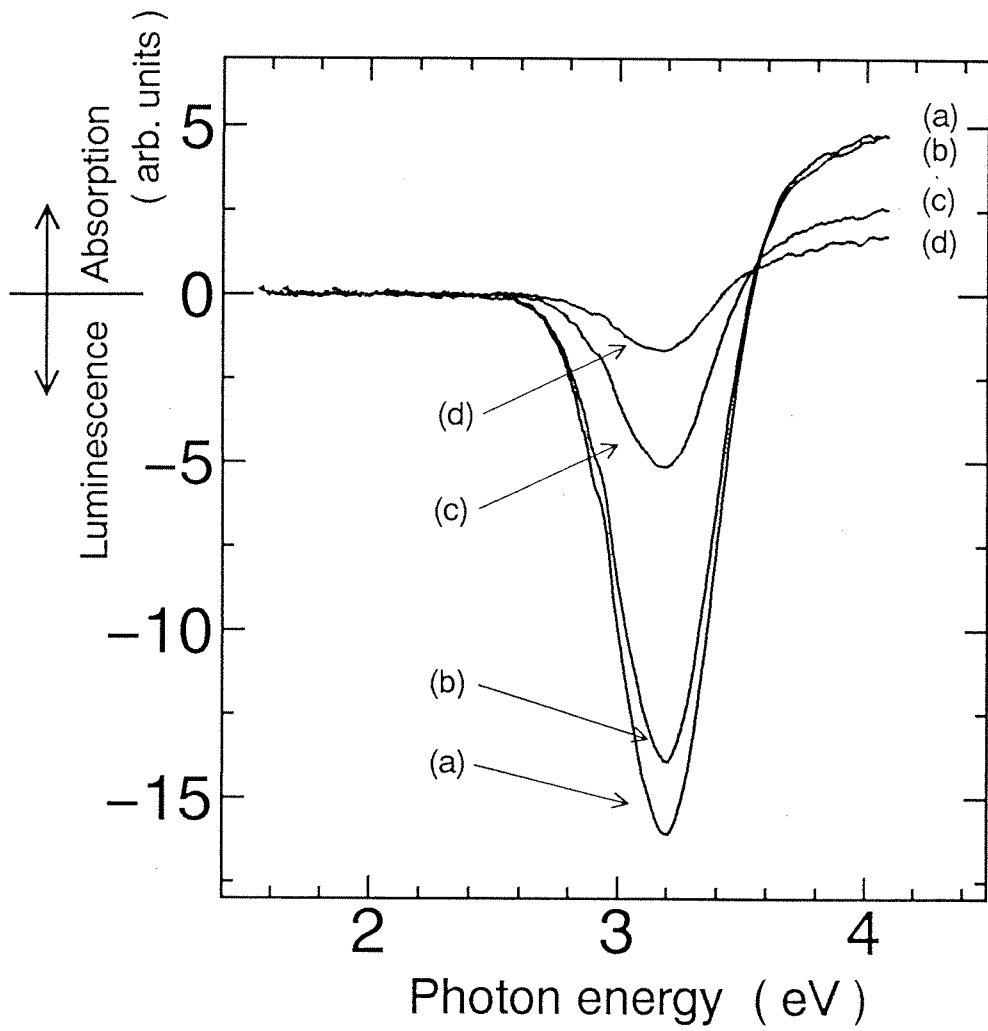
Figure captions:

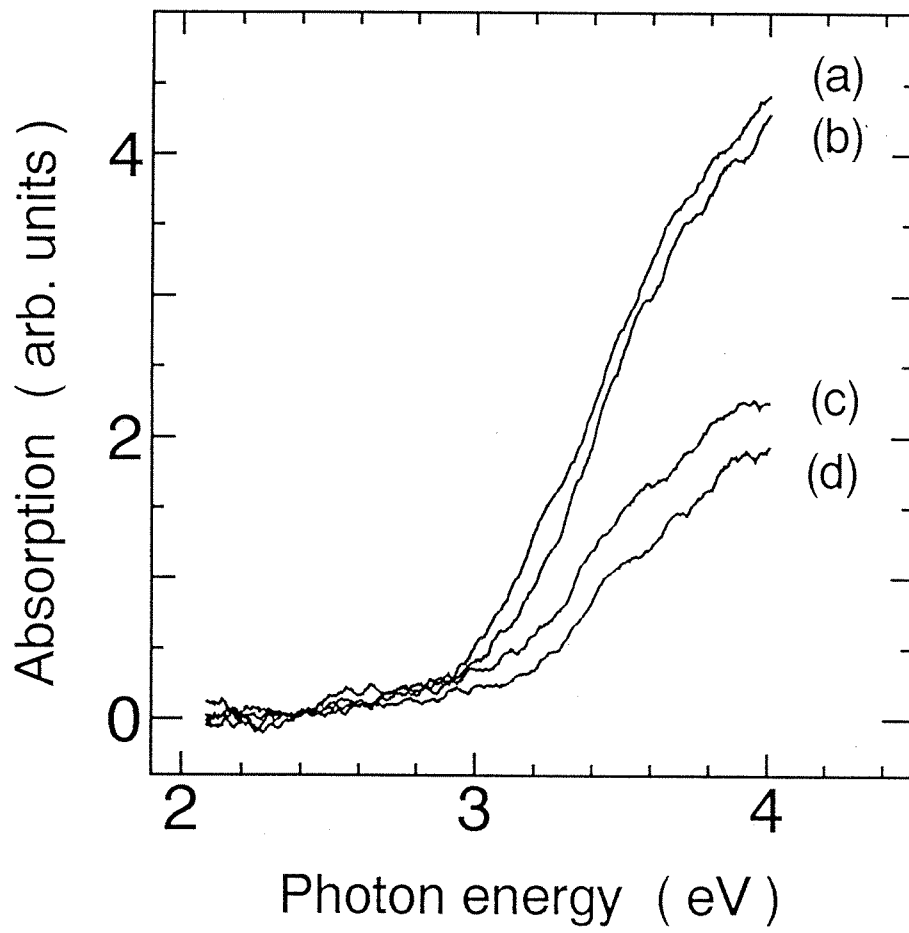
Fig. 1. Time-resolved measurement system for excited-state absorption.

Fig. 2. Observed results of the time-resolved excited-state absorption measurements. The positive hump shows the absorption, while the negative peak shows luminescence. The delay times after the excitation by KrF excimer laser are 100 ns (a), 10 μ s (b), 100 μ s (c), and 200 μ s (d).

Fig. 3. Estimated excited-state absorption spectra. (a)-(d) are the same as indicated in Fig. 2.







Laser-power dependence of absorption changes in Ge-doped SiO₂ glass induced by a KrF excimer laser

Makoto Fujimaki, Kanta Yagi, and Yoshimichi Ohki

Department of Electrical Engineering, Waseda University, 3-4-1 Ohkubo, Shinjuku-ku, Tokyo 169, Japan

Hiroyuki Nishikawa

Department of Electrical Engineering, Tokyo Metropolitan University, 1-1 Minami Osawa, Hachioji, Tokyo 192-03, Japan

Koichi Awazu

Optical Radiation Section, Electrotechnical Laboratory, Umezono, Tsukuba 305, Japan

(Received 13 October 1995)

The generation mechanism of the absorption changes, which cause a photorefractive change through the Kramers-Kronig relation in Ge-doped SiO₂ glass, has not been clarified yet. In the present paper, we examined the laser-power dependence of the absorption changes around 5 eV, induced by a KrF excimer laser. The induced absorption around 5 eV is composed of three different components, centering at 4.50, 5.08, and 5.80 eV. The increasing behavior of each absorption component depends strongly on the energy density. The three absorption components reach different saturation levels, depending on the energy density. Furthermore, the absorption induced by a high-power KrF excimer laser is bleached by a laser, the energy of which density is about one-twentieth of the inducing laser. Combining the results of mathematical analysis, it was found that a two-photon process and a one-photon process are, respectively, involved with the induction and the bleach of each absorption. It was also found that the precursor defect, which causes the absorption change, is of an oxygen-deficient type.

PACS number(s): 42.70.Ce, 42.70.Gi, 42.88.+h

Since the fact that Ge-doped SiO₂ glasses have large absorption bands in the ultraviolet to vacuum ultraviolet (UV-VUV) range was reported, many studies have been done to elucidate the structures responsible for these bands. Especially, the research has been focused on the strong absorption at 5 eV.¹⁻⁶ Through this research, it has become clear that the 5-eV absorption appears only in oxygen-deficient glasses.³ It has been reported that two structures, twofold coordinated germanium⁴ (or germanium lone pair center, GLPC, —Ge—), and neutral oxygen vacancy⁷ (NOV, ≡Ge—T≡), are responsible for this absorption. Here, the symbols “••” and “≡” denote lone-pair electrons and bonds with three separate oxygens, respectively, and *T* is either Ge or Si.

It has been well known that absorption changes are induced in Ge-doped SiO₂ glass, when irradiated by UV photons.^{7,8} Recently, the manufacture of optical filters⁹⁻¹¹ with Bragg gratings in communication fibers was reported. A photorefractive change through the Kramers-Kronig relation induced by some absorption change is utilized for these gratings.¹⁰ Since this was reported, there have been many papers on the absorption changes responsible for the photorefractive change. As the most probable model, the NOV is believed to release one electron and become the *E'* center (≡T⁺+•T≡, *T*: Ge or Si) by absorbing 5-eV photons.⁷ The generation of the germanium electron trapped centers (GEC's) is also responsible for the absorption change.¹¹⁻¹⁴

A discrepancy has been reported for the energy density necessary to make a Bragg grating.¹⁵⁻¹⁷ The difference in efficiency of the generation and bleach of *E'* centers with the energy density of irradiated photons seems to be responsible

for this discrepancy.⁸ It was also reported that the induced absorption shows the saturation at different intensities, depending on the incident energy density.¹⁸ It was further reported that the absorption induced by intense photons is partially bleached when the sample is irradiated by weaker photons.¹⁸ These reports indicate the existence of a certain relation between the absorption change and the energy density, but the details are unknown.

In the present paper, the absorption around 5 eV is very carefully examined, by changing the incident energy density significantly. Based on the observed energy-density dependence of the absorption change, a mathematical analysis is made. The role of a two-photon process and a one-photon process is also discussed.

The samples used are germanium-doped silica glasses of 99SiO₂:1GeO₂ prepared by the vapor-phase axial deposition method. The soot rods were sintered to dense glass rods under reducing atmosphere (H₂:He=1:10). The samples were cut and polished into plates of 0.3 mm thick. Two KrF excimer lasers (248 nm, 5.0 eV) were used as the irradiation photon sources. The one with a higher energy density of 20 to 80 mJ/cm² per pulse (Lambda Physik, LPX105i) is referred to as laser *H*, while the other (MPB Technologies, PSX-100) has an energy density of about 0.5 mJ/cm² per pulse and is called laser *L*. Since the pulse duration of laser *H* is about 20 ns and that of laser *L* is about 5 ns, the average energy density becomes about 1–4 MW/cm² for laser *H* and 100 kW/cm² for laser *L*. The energy density was monitored by a thermopile-type measurement system (Scientech, AD30). The absorption spectra from the visible to UV region were measured by a Shimadzu UV160 spectrophotometer.

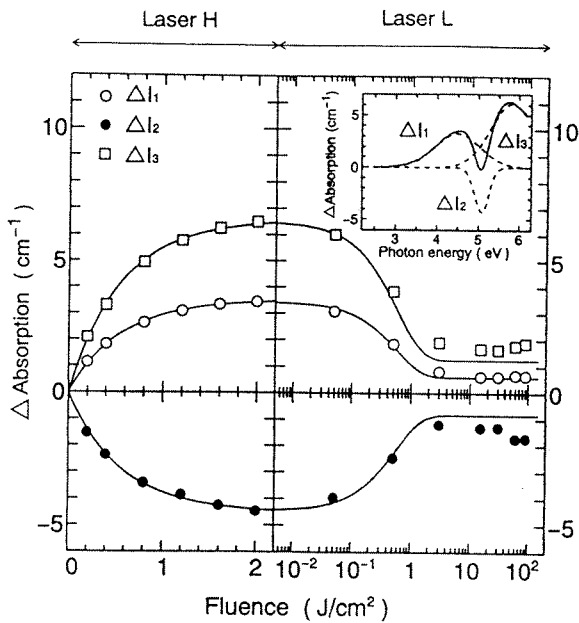


FIG. 1. Change in intensity as a function of fluence for the three absorption components induced by photon irradiation of lasers *H* and *L*. The inset is the induced absorption spectrum by the irradiation of laser *H* of 2 J/cm^2 . \leftrightarrow denotes the period of the irradiation of laser *H*, and \leftrightarrow denotes the period of the irradiation of laser *L* following the irradiation of laser *H*. The energy density of laser *H* used in this experiment is 40 mJ/cm^2 per pulse.

Electron-spin-resonance (ESR) signals were obtained by a JEOL RE-2XG spectrometer at the *X* band frequency. All the experiments were done at room temperature.

Figure 1 shows the change in absorption with fluence observed by the irradiation of intense 5-eV photons. As shown in the inset, the induced absorption is divided into three spectral components with Gaussian line shape, two (ΔI_1 around 4.50 eV and ΔI_3 around 5.80 eV) are positive and the remaining one (ΔI_2 around 5.08 eV) is negative. The peak positions of the three components and their values of the full width at half maximum (FWHM) are shown in Table I. This spectrum is clearly different from the absorption spectrum induced by the irradiation of a Hg/Xe lamp, in which absorption peaks appear at 5 and 6.3 eV.⁷ Although the absorption at 6.3 eV also emerges slowly but clearly, in the present study, after the three absorption changes become saturated at the fluence of about 2 J/cm^2 , this is not the scope of the present paper. Figure 2 shows the dependence of the saturated value of the absorption change on the energy density of laser *H* for the three components. The saturation level is found to depend on the energy density.

TABLE I. Peak positions and values of FWHM of the three absorption components.

	Peak position (eV)	FWHM (eV)
ΔI_1	4.50 ± 0.03	1.31 ± 0.03
$\Delta I_2 (<0)$	5.08 ± 0.01	0.39 ± 0.01
ΔI_3	5.80 ± 0.03	1.27 ± 0.03

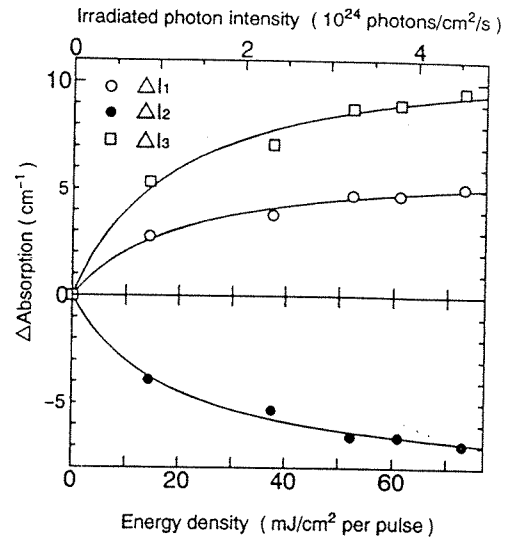


FIG. 2. Change in the saturated absorption intensity induced by laser *H* as a function of the energy density for the three absorption components. The solid curves are drawn by the least-squares fitting to Eq. (7).

As shown in the right half of Fig. 1, the changes in the three absorption components induced by laser *H* are diminished by the ensuing photon irradiation by laser *L*. The three components approach to their respective stable levels when the total fluence by laser *L* reaches about 4 J/cm^2 . These data indicate that the reaction, which causes the absorption changes, is an equilibrium reaction between the inducing and the bleaching processes.

The inset in Fig. 3 shows the ESR spectrum induced by the irradiation of 2 J/cm^2 by laser *H*. The spectrum is very close to what is believed to be due to the GEC's,¹⁹ although the assignment is still debatable.¹⁴ Figure 3 shows a good proportionality between the intensity of each induced absorption component and the density of the induced paramagnetic

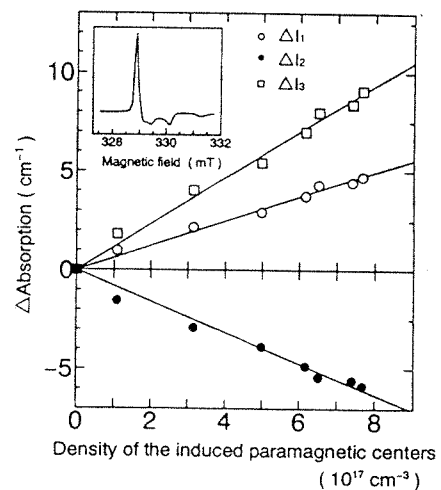
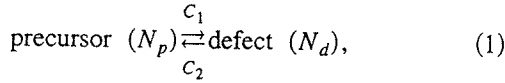


FIG. 3. Dependence of the intensity for three absorption components induced by the irradiation of up to 2 J/cm^2 by laser *H*, on the density of induced paramagnetic defect centers. The inset shows the ESR spectrum of the induced paramagnetic centers.

defect centers. That is to say, the absorption around 4.50 eV (ΔI_1) and the one around 5.80 eV (ΔI_3) are induced concomitantly with the decrease of the absorption around 5.08 eV (ΔI_2), keeping the ratios $\Delta I_1/\Delta I_2$ and $\Delta I_3/\Delta I_2$ constant. This strongly suggests that the defect responsible for ΔI_2 is converted to the defect(s) responsible for ΔI_1 and ΔI_3 . Namely, ΔI_2 is caused by the precursor defect and ΔI_1 and ΔI_3 are caused by the induced defect(s).

As already mentioned, the results of Figs. 1 and 2 suggest that the behavior of the absorption change is determined by the equilibrium between the inducing and the bleaching processes, as expressed by the following:



where $c_1(s^{-1})$ and $c_2(s^{-1})$ are rate constants. Then, we start with a first-order kinetic equation involving both the forward and the backward reactions as follows:

$$\frac{dN_p}{dt} = -c_1 N_p + c_2 N_d, \quad (2a)$$

$$N_p + N_d = N_0, \quad (2b)$$

$$N_p(t=0) = N_0, \quad N_d(t=0) = 0. \quad (2c)$$

Here, we define N_p and N_d as the numbers of precursor defects and induced defects, respectively. N_0 is the initial number of N_p . The solution of these equations is given by

$$N_d = N_0 - N_p = \frac{c_1}{c_1 + c_2} N_0 \{1 - \exp[-(c_1 + c_2)t]\}. \quad (3)$$

The numbers of the defects, N_p and N_d , will be saturated as follows:

$$N_d(t \rightarrow \infty) = N_0 - N_p(t \rightarrow \infty) = \frac{c_1}{c_1 + c_2} N_0. \quad (4)$$

If we assume, for example, that both the inducing and the bleaching processes are governed by respective one-photon processes, i.e., if the rate constants c_1 and c_2 are both proportional to the incident energy density, the value of $N_d(t \rightarrow \infty)$ should be constant. Contrary to this, however, the saturation values vary with the incident energy density, as shown in Fig. 2. Nishii *et al.*^{12,20} reported that the formation of the GEC's, which are responsible for UV absorption bands, is caused by a two-photon process. Furthermore, we have confirmed that the absorption change shown in the inset of Fig. 1 does not occur when a Hg/Xe lamp is used as a light source. Therefore, we assume the following relations between the rate constants and the incident energy density:

$$c_1 = \alpha P^2 \quad (\text{two-photon process}), \quad (5a)$$

$$c_2 = \beta P \quad (\text{one-photon process}), \quad (5b)$$

where P ($\text{cm}^{-2} \text{s}^{-1}$) denotes the number of incident photons per unit area per second, which corresponds to the incident energy density, and α ($\text{cm}^4 \text{s}$) and β (cm^2) are constants. Therefore, we obtain the following relations for N_p and N_d from Eq. (3):

TABLE II. Constants α and β for lasers \underline{H} and \underline{L} .

	α ($\text{cm}^4 \text{s}$)	β (cm^2)
Inducing period		
by laser H	0.39×10^{-42}	0.49×10^{-18}
Diminishing period		
by laser L	1.0×10^{-42}	1.3×10^{-18}

$$N_d = N_0 - N_p = \frac{\alpha}{\alpha + \beta/P} N_0 \{1 - \exp[-(\alpha P^2 + \beta P)t]\}. \quad (6)$$

From Eq. (4), the dependencies of $N_p(t \rightarrow \infty)$ and $N_d(t \rightarrow \infty)$ on the incident energy density are as follows:

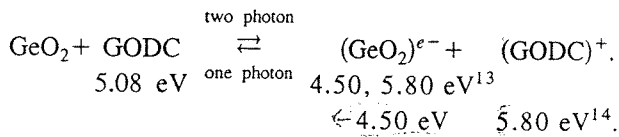
$$N_d(t \rightarrow \infty) = N_0 - N_p(t \rightarrow \infty) = \frac{\alpha}{\alpha + \beta/P} N_0. \quad (7)$$

While ΔI_1 and ΔI_3 are proportional to the number(s) of the corresponding induced defects (N_d), ΔI_2 is proportional to the number of the precursor defects, which have changed to the induced defects ($N_p - N_0$). Therefore, all the three absorption components can be calculated from Eq. (6). The solid curves, in the left half of Fig. 1, are drawn by assuming Eq. (6). Closely tracing the theoretical curves, the values ΔI_1 , ΔI_2 , and ΔI_3 approach to their respective saturation values. If, at this moment, the photon source is changed to laser L from laser H , the numbers of both defects again begin to approach to their respective saturation values. The absorption change in this period can be calculated similarly from Eq. (2a), by assuming that the saturation values of N_d and N_p of the previous period (namely, by laser H) are their initial values of this period. Solid curves in the right half of Fig. 1 are drawn in this way. Furthermore, the solid curves in Fig. 2 representing the change in the saturated absorption intensity induced by laser H are drawn by assuming Eq. (7). The fact that the experimental data in Figs. 1 and 2 are fitted very well by these solid curves suggests the validity of our assumed model.

The constants α and β , or the efficiency of the two-photon process and that of the one-photon process, should be independent of the energy density of irradiated photons. Table II shows the values of α and β used through the calculations for the inducing period by laser H and for the diminishing period by L . The difference of α between the inducing period and the diminishing period is about a factor of 2.6. So is the difference of β . If the difference in shape of the photon pulses from the two lasers and inevitable shot-to-shot differences are taken into account, such a difference can be considered to be small enough to indicate that both α and β are independent of the energy density. This strengthens the validity of our assumed model.

From these results, it has been confirmed that the defect responsible for the absorption around 5.08 eV is converted by a two-photon process to the defect(s) responsible for the absorption around 4.50 and 5.80 eV and that its backward

reaction occurs by a one-photon process. From Fig. 3, it is obvious that the 5.08 eV absorption band is the precursor of the GEC, and that either of the induced absorption bands at 4.50 and 5.80 eV or both are assigned to the GEC. One important fact that should be remembered is that the absorption at 5.08 eV is observed only in the oxygen-deficient-type Ge-doped SiO₂ glass. Therefore, the absorption at 5.08 eV should be assigned to a germanium oxygen-deficient center (GODC), no matter whether it is GLPC,⁴ NOV,⁷ or any other form,²¹ or a combination thereof. The assignment of the absorption bands at 4.50 and 5.80 eV has been discussed in several papers. While the 4.50 eV (4.4 eV in Ref. 13) and the 5.80 eV bands are assigned to two types of GEC's, Ge(1) and Ge(2), respectively, in Ref. 13, the two bands are assigned to the GEC and the positively charged GODC, respectively, in Ref. 14. Combining these assignments with the results of the present study, the mechanism of the absorption change is expressed as follows:



Here (GeO₂)^{e-} can be referred to as GEC. More analyses such as on the structural assignment of GODC will continue in a future paper.

In the right half of Fig. 1, it is observed that the experimental data of ΔI₂ decreases and ΔI₃ increases again with the irradiation of laser L, when the irradiation of laser L exceeds 4 J/cm². This phenomenon is understood if the gen-

eration of the E' center is taken into account. It has been reported that the irradiation of UV photons breaks the NOV into E' center and that this phenomenon is accompanied by the absorption decrease around 5 eV and the absorption increase around 6.3 eV.^{7,22} As already mentioned, we have confirmed that this phenomenon becomes obvious with the prolonged irradiation of photons, thus putting ΔI₂ and ΔI₃ below and above the calculated curves, respectively.

Since the photorefractive index change in Ge-doped SiO₂ glasses is induced effectively by the irradiation of intense photons at 5 eV,^{8,12,22} and the absorption change should be closely related with photorefractive index change through the Kramers-Kronig relation,^{11,12,22} the present findings are very important. Furthermore, that the induced absorption changes are diminished by one-photon absorption of 5-eV photons is a negative factor for the utilization of the photorefractive effect.

To conclude, as for the absorption change, which consists of the induction of absorption bands at 4.50 and 5.80 eV and the bleaching of 5.08-eV absorption induced in Ge-doped SiO₂ glass by irradiation of 5-eV photons, a two-photon process at oxygen-deficient centers is responsible. The backward process is caused by a one-photon process.

We thank Dr. K. Muta and Ms. M. Kato of Showa Electric Wire and Cable Company, Ltd., for supplying the samples. This work was partly supported by a Grant-in-Aid for Scientific Research from the Ministry of Education, Science and Culture of Japan (06452222), and by a Grant-in-Aid for Promoted Research by Young Researchers from Tokyo Metropolitan University.

- ¹L. Skuja, *J. Non-Cryst. Solids* **149**, 77 (1992).
- ²J. Wong and C. A. Angell, *Glass Structure by Spectroscopy* (Marcel Dekker, New York, 1976), Chap. 5.
- ³M. Kohketsu, K. Awazu, H. Kawazoe, and M. Yamane, *Jpn. J. Appl. Phys.* **28**, 622 (1989).
- ⁴M. J. Yuen, *Appl. Opt.* **21**, 136 (1982).
- ⁵M. Gallagher and U. Osterberg, *J. Appl. Phys.* **74**, 2771 (1993).
- ⁶K. Awazu, H. Kawazoe, and M. Yamane, *J. Appl. Phys.* **68**, 2713 (1990).
- ⁷H. Hosono, Y. Abe, D. L. Kinser, R. A. Weeks, K. Muta, and H. Kawazoe, *Phys. Rev. B* **46**, 11 445 (1992).
- ⁸T. E. Tsai, C. G. Askins, and E. J. Friebele, *Appl. Phys. Lett.* **61**, 390 (1992).
- ⁹K. O. Hill, Y. Fujii, D. C. Johnson, and B. S. Kawasaki, *Appl. Phys. Lett.* **32**, 647 (1978).
- ¹⁰R. M. Atkins and V. Mizrahi, *Electron. Lett.* **28**, 1743 (1992).
- ¹¹D. L. Williams, S. T. Davey, R. Kashyap, J. R. Armitage, and B. J. Ainslie, *Electron. Lett.* **28**, 369 (1992).
- ¹²J. Nishii, N. Kitamura, H. Yamanaka, H. Hosono, and H. Kawazoe, *Opt. Lett.* **20**, 1184 (1995).
- ¹³E. J. Friebele and D. L. Griscom, in *Defects in Glasses*, edited by F. L. Galeener, D. L. Griscom, and M. J. Weber, *MRS Symposia Proceedings No. 61* (Materials Research Society, Pittsburgh, 1986) p. 319.
- ¹⁴E. V. Anokin, A. N. Guryanov, D. D. Gusovsky, V. M. Mashinsky, S. I. Miroshnichenko, V. B. Neustruev, V. A. Tikhomirov, and Yu. B. Zverev, *Sov. Lightwave Commun.* **1**, 123, (1991).
- ¹⁵G. Meltz, W. Morely, and W. H. Glenn, *Opt. Lett.* **14**, 823 (1989).
- ¹⁶E. Fertein, S. Legoubin, M. Douay, S. Cannon, P. Bernage, and P. Niy, *Electron. Lett.* **27**, 1838 (1991).
- ¹⁷B. Malo, K. A. Vineberg, F. Bilodean, J. Albert, D. C. Johnson, and K. O. Hill, *Opt. Lett.* **15**, 953 (1990).
- ¹⁸V. B. Neustruev, E. M. Dianov, V. M. Kim, V. M. Mashinsky, M. V. Romanov, A. N. Guryanov, V. F. Khopin, and V. A. Tikhomirov, *Fiber Integrated Opt.* **8**, 143 (1989).
- ¹⁹Y. Watanabe, H. Kawazoe, K. Shibuya, and K. Muta, *Jpn. J. Appl. Phys.* **25**, 425 (1986).
- ²⁰J. Nishii, K. Fukumi, H. Yamanaka, K. Kawamura, H. Hosono, and H. Kawazoe, *Phys. Rev. B* **52**, 1661 (1995).
- ²¹T. E. Tsai and E. J. Friebele, *Appl. Phys. Lett.* **64**, 1481 (1994).
- ²²L. Dong, J. L. Archambault, L. Reekie, P. St. J. Russell, and D. N. Payne, *Appl. Opt.* **34**, 3436 (1995).

Photoluminescence study on point defects in buried SiO₂ film formed by implantation of oxygen

Kwang Soo Seol,^{a)} Akihito Ieki, and Yoshimichi Ohki

Department of Electrical Engineering, Waseda University, 3-4-1 Ohkubo, Shinjuku-ku, Tokyo 169, Japan

Hiroyuki Nishikawa

Department of Electrical Engineering, Tokyo Metropolitan University, 1-1 Minami-Osawa, Hachioji, Tokyo 192-03, Japan

Masaharu Tachimori

Advanced Semiconductor Technology Laboratory, Nippon Steel Corporation, 5-10-1 Fuchinobe, Sagamihara, Kanagawa 229, Japan

(Received 11 April 1995; accepted for publication 6 September 1995)

Defects in buried SiO₂ films in Si formed by implantation of oxygen ions were characterized by photoluminescence (PL) excited by KrF (5.0 eV) excimer laser and synchrotron radiation. Two PL bands were observed at 4.3 and 2.7 eV. The 4.3 eV band has two PL excitation bands at 5.0 and 7.4 eV, and its decay time is 4.0 ns for the 5.0 eV excitation and 2.4 ns for the 7.4 eV excitation. The decay time of the 2.7 eV PL band is found to be 9.7 ns. These results are very similar to those for the 4.3 eV and the 2.7 eV PL bands, which are observed in bulk silica glass of an oxygen-deficient type and attributed to the oxygen vacancy. Through the change in the PL intensity with the film thickness, the buried SiO₂ film is considered to contain the oxygen vacancy defects in a high amount throughout the oxide. © 1996 American Institute of Physics. [S0021-8979(95)03424-3]

I. INTRODUCTION

With the development of high-speed and high-power devices, the parasitic capacitance and the lateral insulation have become serious problems. To solve these problems, various fabrication methods for a silicon-on-insulator structure were developed. Among these developed methods, formation of an oxide layer in a monocrystalline silicon by implantation of high-energy oxygen ions is thought to be the most competitive for mass production. This is usually referred to as separation by implanted oxygen (SIMOX).

However, there have recently been a number of deviating observations on devices with SIMOX buried oxides, which are induced by unusual behavior of the buried oxide such as enhanced electrical conductivity,¹ charge buildup,^{2,3} and significantly enhanced sensitivity⁴⁻⁶ to defect generation as compared to the conventional thermal oxide. It is suggested that there is a distinct difference between the two oxides in such points as structure, uniformity and the degree of nonstoichiometry.

From such a viewpoint, much research has been done recently on the properties of SIMOX.¹⁻⁸ Electron spin resonance (ESR) always gives useful information on the structure of paramagnetic defects such as E' center ($\equiv\text{Si}\cdot$; " \equiv " and " \cdot " denote bonds with three separate oxygens and an unpaired electron, respectively) and the nonbridging oxygen hole center ($\equiv\text{Si}-\text{O}\cdot$).⁹⁻¹¹ Diamagnetic defects, which act as precursors of paramagnetic centers, cannot be detected by ESR. On the other hand, photoluminescence (PL) has been proved to be a powerful tool to characterize diamagnetic defects in bulk silica glasses.¹²⁻¹⁴

Recently, characterization of various silicon oxide thin films by PL has been tried,¹⁵⁻¹⁷ but not yet for SIMOX bur-

ied oxide film. In addition to that, SIMOX wafer is now examined on the applicability to novel optical devices, which utilize low-dimensional silicon structure.^{18,19} If there are uncertain PLs from the SIMOX buried oxide film, the exact characterization of the low-dimensional silicon should become difficult.

In this study we report on a PL study on point defects in SIMOX buried oxides, based on PL and PL excitation (PLE) spectra and decay characteristics obtained with excimer laser photons and synchrotron radiation.

II. EXPERIMENT

The SIMOX buried oxides (hereafter abbreviated as SIMOX) were produced by implanting O⁺ ions up to a dose of 1.7×10^{18} ions/cm² with an energy of 180 keV into *p*-type (100) Si substrates maintained at 550 °C. The substrates were then annealed at 1300 °C in Ar+O₂ for 6 h. For PL experiment, the Si overlayer was etched off in a KOH solution [KOH:H₂O=3.7 (by weight)] stabilized at 23 °C to expose the buried oxide. The buried oxide was etched back in buffered (10:1) HF acid solution to change the thickness. The oxide thickness was measured by ellipsometry with He-Ne laser (632.8 nm). For comparison, the following three kinds of oxide were used. The first one, abbreviated as pure silica, is a high-purity oxygen-deficient-type bulk SiO₂ glass ([OH]: 3 ppm, [Cl]: 670 ppm) prepared by the Ar plasma method. The second one is a wet-type thermal oxide prepared by oxidation of a *p*-type Si substrate in a wet oxygen atmosphere at 1000 °C for 70 min. The third one is a phosphorous-implanted thermal oxide prepared by implanting P⁺ ions with an energy of 80 keV up to 10^{16} ions/cm² into thermal oxide.

The PL spectra were measured using a monochromator (Jobin-Yvon HR320) equipped with a multichannel detector

^{a)}Electronic mail: 695c5056@cfi.waseda.ac.jp

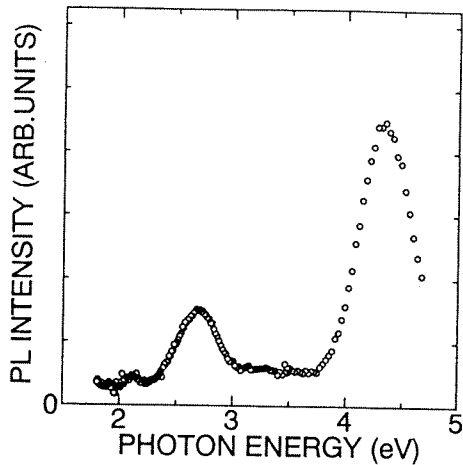


FIG. 1. Photoluminescence spectrum at room temperature from SIMOX oxide when excited by a KrF excimer laser (5.0 eV).

(Princeton RY-1024) and the ns-order decay profiles were measured with a photomultiplier (Hamamatsu R955) under excitation by a KrF excimer laser [wavelength: 248 nm (5.0 eV); pulse width: ~ 20 ns; pulse energy: 10–20 mJ/cm², Lambda Physik LPX105i).

The PLE spectra and ns-order decay profiles were measured using synchrotron radiation (SR) at the BL7B line of UVSOR operated at an electron energy of 750 MeV (Institute for Molecular Science, Okazaki, Japan). While the PLE spectra were measured under multibunch operation, the decay profiles were measured by a time-correlated single-photon counting technique under single-bunch operation (time interval of SR pulses: 177.6 ns). An apparent pulse duration of the SR pulse including time response of the detecting system is 0.55 ns. The emitted photons collected with a lens at 30° or 90° to the incident beam and dispersed by a bandpass filter were detected by a photomultiplier (Hamamatsu R955) for PLE or by a microchannel-plate photomultiplier (Hamamatsu R2287U-06) for the decay. Measurement were carried out at 32–300 K.

III. RESULTS

Shown in Fig. 1 is the PL spectrum of SIMOX obtained under excitation by the KrF excimer laser at room temperature. Two PL bands are observed at 4.3 and 2.7 eV. Here, the spectrum below 3.5 eV was taken with a filter to remove an artifact peak around 2.2 eV arising from second-order light of the 4.3 eV PL.

Figure 2 shows the PLE spectrum for the 4.3 eV PL band obtained with synchrotron radiation. Here, the obtained luminescence intensity was divided by the intensity of the excitation photons, and the measurement was done at 90 K. A clear PLE band is seen at 7.4 eV. On the steep increase beginning around 5.4 eV, which is due to scattered excitation photons through the bandpass filter with a transmittance window at 4.3 eV, a shoulder is seen around 5.0 eV. As is confirmed below, this shoulder is thought to be a PLE peak of the 4.3 eV band.

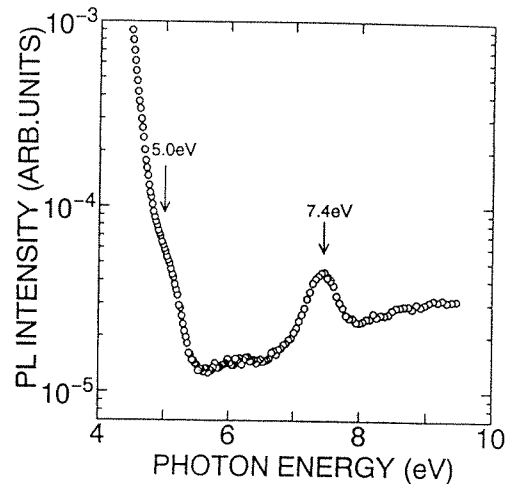
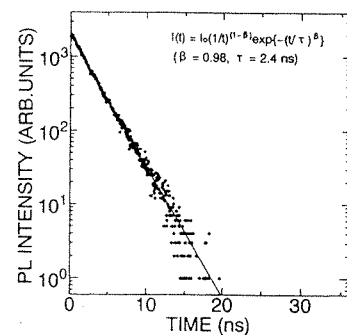


FIG. 2. Photoluminescence excitation spectrum obtained at 90 K for the 4.3 eV PL band in SIMOX oxide.

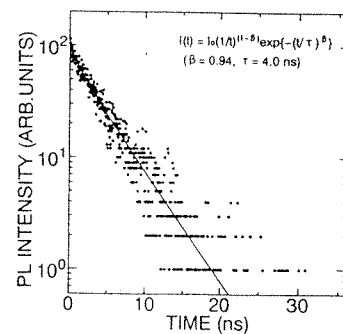
Figure 3 shows the decay of the 4.3 eV PL excited at (a) 7.4 eV and (b) 5.0 eV for SIMOX, measured at 32 K. The data were fitted by the least-squares method with the time derivative of a stretched exponential function,

$$I(t) \propto (\beta/\tau)(\tau/t)^{1-\beta} \exp[-(t/\tau)^\beta]. \quad (1)$$

Here τ and β are the effective decay constant and a parameter which takes a value of $0 < \beta < 1$, respectively. This is



(a) Excited by 7.4 eV photons



(b) Excited by 5.0 eV photons

FIG. 3. Decay profiles of the 4.3 eV PL band excited at (a) 7.4 eV and (b) 5.0 eV for SIMOX oxide. Solid curves are drawn by assuming the stretched exponential function, Eq. (1).

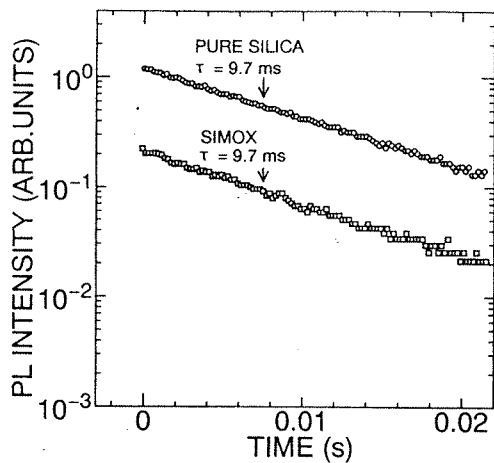


FIG. 4. Decay profiles of the 2.7 eV PL band from oxygen-deficient pure silica and SIMOX oxide.

consistent with many reports which revealed that the luminescence decay in many amorphous materials measured below 50 K is described by the above equation.²⁰⁻²²

Figure 4 compares the decay of the 2.7 eV PL band of SIMOX and that of pure silica. The PL was excited by the KrF excimer laser and measured at room temperature. In both two samples, the PL decays exponentially with the same decay constant of 9.7 ms.

The thickness of SIMOX was changed by etching with HF solution. Figure 5 shows the change in height of the 4.3 eV PL band with the remaining thickness. The PL intensity depends linearly on the thickness.

IV. DISCUSSION

Study on PL has been offering a strong clue to the characterization of high-purity or Ge-doped silica glass for optical communication;^{12-14,23} however, such PL study has rarely been used for the study of thin SiO₂ film.^{15-17,24} This is

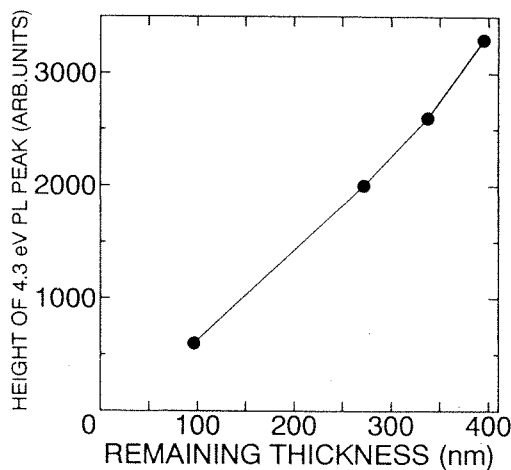


FIG. 5. Change in the height of 4.3 eV PL peak with the remaining thickness of SIMOX oxide.

partly due to the experimental difficulty in obtaining data with a high signal-to-noise ratio in the vacuum-ultraviolet range. Recently, we surmounted this difficulty by using synchrotron radiation and reported PL from SiO₂ films deposited by plasma-enhanced chemical-vapor deposition and ion-implanted thermal SiO₂ films.^{15,17}

Among many PL bands observed in high-purity silica, two PL bands at 4.3 and 2.7 eV are the best-characterized bands. When they appear simultaneously like a geminate pair in one sample, and if the sample has two absorption bands around 5.0 and 7.6 eV, the sample can be considered to be oxygen deficient.^{12,25-27} The 4.3 eV PL band in the oxygen-deficient silica glass has a decay constant of 4.2 ns for the 5.0 eV excitation and that of 2.1 ns for the 7.6 eV excitation,²⁷ while the 2.7 eV PL band has a decay constant around 10 ms.^{12,28,29} These are in good agreement with the results shown in Figs. 1-4, except for some subtle differences like the existence of PLE band at 7.4 eV rather than at 7.6 eV. A slight shift in the peak energy of the PLE band often occurs, since electronic excitation is influenced by the surrounding atmosphere of the point defect. We found that ion-implanted thermal SiO₂ films also have the corresponding PLE band at 7.4 eV.¹⁷ Therefore, all the obtained results indicate that the present SIMOX oxide is oxygen deficient in nature. This is to say, the PL pair at 4.3 and 2.7 eV and the absorption (PLE) pair at 5.0 and 7.4 eV are due to the same point defects as in the case of bulk silica glass, and not due to the quantum effect of small silicon islands,³⁰ which may exist in SIMOX oxide.

One point we want to mention here is that the PL peak position alone could not be so decisive, although PL study is indeed a powerful tool to characterize the material. One example is that PL appeared at 2.6 eV when SIMOX was irradiated by an ArF excimer laser whose photon energy is 6.4 eV.³¹ Although the peak position is close to the 2.7 eV PL, the decay constant, which is shorter than 100 μs, is completely different from that of the 2.7 eV PL. Therefore, attention should also be paid to the PLE spectra and the decay constant in addition to the peak position. Detailed study on the 2.6 eV band and another PL at 3.3 eV, which was also observed under the ArF excimer laser, will be our future task.

As for the structure of the point defects responsible for the PL pair and the PLE pair, mainly the following two models are considered. One is the oxygen-deficient-center (ODC) model. In this model, the 7.6 eV absorption is due to "relaxed" (i.e., with shortened bond) oxygen vacancy ($\equiv\text{Si}-\text{Si}\equiv$), while the 5.0 eV absorption is due to "unrelaxed" (i.e., holding the longer bond) oxygen vacancy.³² The corresponding PLs at 4.3 and at 2.7 eV are considered to be due to electronic transition to the ground (singlet) state from the excited singlet state and that from the triplet state, respectively.²⁸ The other model is the silicon-lone-pair-center (SLPC) model. This model assumes that the twofold coordinated Si (O- $\ddot{\text{S}}\text{i}$ -O, "... denotes lone-pair electrons) for the 5.0 eV band and impurity-related (hydrogen and/or chlorine) complex defects of the twofold coordinated silicon for the 7.6 eV band.³³ Between the two models, the ODC model seems more favorable, since the 7.4 eV PLE, which corresponds to the 7.6 eV absorption, is observed in SIMOX,

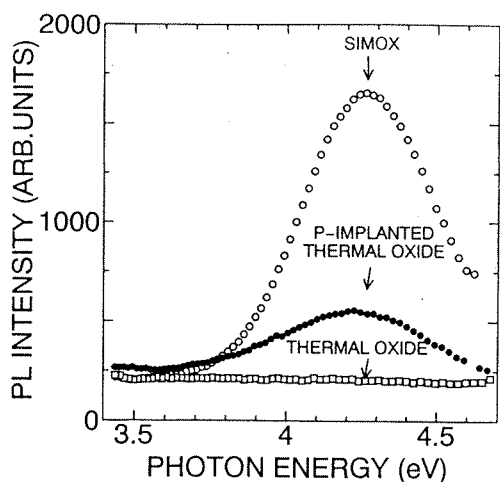


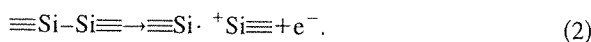
FIG. 6. Comparison of the photoluminescence spectra from SIMOX oxide (400 nm), P-implanted thermal oxide (110 nm), and thermal oxide (500 nm).

in which neither hydrogen nor chlorine is assumed to be introduced during the manufacture. As mentioned above, we observed the 7.4 eV PLE band in ion-implanted thermal SiO₂ films.¹⁷ This fact is also unfavorable for the SLPC model. Consequently, together with the result shown in Fig. 5, oxygen vacancies are thought to exist almost uniformly throughout the oxide.

As shown in Fig. 3, the values of τ and β for the 4.3 eV PL are 2.4 ns and 0.98, respectively for the 7.4 eV excitation, and 4.0 ns and 0.94, respectively for the 5.0 eV excitation. The stretched exponential function [Eq. (1)] becomes single exponential if $\beta=1$. The value of 0.98 or 0.94 is close to 1. Therefore, the present result is consistent with our previous work for oxygen-deficient silica glass, in which we reported that the 4.3 eV PL shows a single-exponential decay with $\tau=2.1$ ns under the excitation of 7.6 eV photons and that with $\tau=4.2$ ns under the excitation of 5.0 eV photons.²⁷ In the case of the 4.3 eV PL in thin SiO₂ films formed by plasma-enhanced chemical-vapor deposition (CVD) of tetraethoxysilane, β is well below 1 ($\beta=0.78$) when excited at 7.6 eV, although τ is not so different ($\tau=2.8$ ns).¹⁵ Lower β means that the function deviates more from a single-exponential decay, and it is an indication of structural distortion surrounding the point defect. From this point of view, the structure of SIMOX buried oxide can be assumed to be similar to high-purity silica glass formed by the conventional CVD-soot remelting method,²⁷ and much more uniform than plasma CVD SiO₂ from tetraethoxysilane.¹⁵

Finally, we want to discuss the reason for the deviating behavior of devices with SIMOX buried oxide such as the enhanced sensitivity to defect generation under irradiation.⁴⁻⁶ The PL spectra around 4.3 eV from SIMOX (thickness: 400 nm), thermal oxide (500 nm), and P-implanted thermal oxide (110 nm) excited by the KrF excimer laser are shown in Fig. 6. As clearly seen, SIMOX contains oxygen vacancies nearly as much as P-implanted thermal oxide (note the difference in thickness) and far more than thermal oxide. The oxygen vacancy is known to act as a

precursor of the E' center and an electron supplier through the equation.³⁴



Therefore, the abundance of oxygen vacancies in SIMOX buried oxide seems to be responsible for the high sensitivity to defect generation, the high conductivity, or the charge buildup.

V. CONCLUSIONS

We observed photoluminescence from SIMOX buried oxide and obtained the following results.

(1) Under the excitation of KrF excimer laser, two PL bands at 4.3 and 2.7 eV are observed. Using synchrotron radiation, it is confirmed that the 4.3 eV PL has two PLE bands at 5.0 and 7.4 eV. These PLs and PLEs are considered to be due to the oxygen vacancies existing almost uniformly in the oxide.

(2) The structure surrounding the oxygen vacancy, judged by the small deviation of the PL decay curve from a single exponential one, is similar to that of high-purity silica glass.

(3) By comparison of the intensities of the 4.3 eV PL, it is found that the density of oxygen vacancy in SIMOX buried oxide is by far higher than thermal silicon oxide. This seems to be a reason of deviating behavior of SIMOX.

ACKNOWLEDGMENTS

The authors express their thanks to Dr. K. Ishii of Waseda University and M. Takiyama of Nippon Steel Corporation for valuable discussion. This work was partly supported by a Grant-in-Aid (No. 06452222) from the Ministry of Education, Science, and Culture of Japan, a Grant-in-Aid for Special Research Project from Tokyo Metropolitan University (1994), the Casio Science Promotion Foundation, and the Joint Studies Program (1992-1994) of UVSOR Facility, Institute for Molecular Science, Okazaki, Japan.

¹G. A. Brown and A. G. Revesz, IEEE Trans. Electron Devices **ED-40**, 1700 (1993).

²N. K. Annamalai, J. F. Bockman, N. E. McGruer, and J. Chapski, IEEE Trans. Nucl. Sci. **NS-37**, 2001 (1990).

³H. Boesch, T. Taylor, and G. Brown, IEEE Trans. Nucl. Sci. **NS-38**, 1234 (1991).

⁴A. Stesmans, R. Devine, A. G. Revesz, and H. Hughes, IEEE Trans. Nucl. Sci. **NS-37**, 2008 (1990).

⁵A. Stesmans and K. Vanheusden, Appl. Phys. Lett. **62**, 2277 (1993).

⁶R. A. B. Devine, J.-L. Leray, and L. Margail, Appl. Phys. Lett. **59**, 2275 (1991).

⁷K. Vanheusden and A. Stesmans, Appl. Phys. Lett. **57**, 2250 (1990).

⁸K. Vanheusden and A. Stesmans, J. Appl. Phys. **69**, 6656 (1991).

⁹D. L. Griscom, in *Defects in Glasses*, edited by F. L. Galeener, D. L. Griscom, and M. J. Weber, MRS Symposium Proceedings No. 61 (MRS, Pittsburgh, 1986), p. 213.

¹⁰D. L. Griscom, Rev. Solid State Sci. **4**, 565 (1990).

¹¹H. Nishikawa, R. Thomon, Y. Ohki, K. Nakasawa, and Y. Hama, J. Appl. Phys. **65**, 4672 (1989).

¹²H. Nishikawa, T. Shiroshima, R. Nakamura, Y. Ohki, K. Nagasawa, and Y. Hama, Phys. Rev. B **45**, 586 (1992).

¹³L. Skuja, J. Non-Cryst. Solids **149**, 77 (1992).

¹⁴J. H. Stathis and M. A. Kastner, Phys. Rev. B **35**, 2972 (1987).

- ¹⁵ K. Ishii, Y. Ohki, and H. Nishikawa, *J. Appl. Phys.* **76**, 5418 (1994).
- ¹⁶ T. Kanashima, R. Nagayoshi, M. Okuyama, and Y. Hamakawa, *J. Appl. Phys.* **74**, 5742 (1993).
- ¹⁷ H. Nishikawa, E. Watanabe, D. Ito, M. Takiyama, A. Ieki, and Y. Ohki (unpublished).
- ¹⁸ G. Hashiguchi and H. Mimura, *Jpn. J. Appl. Phys.* **33**, L1649 (1994).
- ¹⁹ Y. Takahashi, T. Furuta, T. Ishiyama, and M. Tabe, in *Extended Abstracts of the 1994 International Conference on Solid State Devices and Materials*, Yokohama, p. 748.
- ²⁰ K. Murayama and T. Ninomiya, *Jpn. J. Appl. Phys.* **21**, L512 (1982).
- ²¹ K. Murayama and T. Ninomiya, *Solid State Commun.* **53**, 125 (1985).
- ²² K. M. Hong, J. Noolandi, and R. A. Street, *Phys. Rev. B* **23**, 2967 (1981).
- ²³ L. Skuja, *J. Non-Cryst. Solid* **164**, 229 (1994).
- ²⁴ K. Awazu, K. Watanabe, and H. Kawazoe, *Jpn. J. Appl. Phys.* **32**, 2746 (1993).
- ²⁵ C. M. Gee and M. A. Kastner, *Phys. Rev. Lett.* **42**, 1765 (1979).
- ²⁶ R. Tohmon, H. Mizuno, Y. Ohki, K. Sasagane, K. Nagasawa, and Y. Hama, *Phys. Rev. B* **39**, 1337 (1989).
- ²⁷ H. Nishikawa, E. Watanabe, D. Ito, and Y. Ohki, *Phys. Rev. Lett.* **72**, 2101 (1994).
- ²⁸ R. Thomon, Y. Shimogaichi, H. Mizuno, Y. Ohki, K. Nagasawa, and Y. Hama, *Phys. Rev. Lett.* **62**, 1388 (1989).
- ²⁹ C. M. Gee and M. Kastner, in *The Physics of MOS Insulators*, edited by G. Lukovsky, S. T. Pantelides, and F. L. Galeener (Pergamon, New York, 1980), p. 132.
- ³⁰ D. J. DiMaria, J. R. Kirtley, E. J. Pakulis, D. W. Dong, T. S. Kuan, F. L. Pesavento, T. N. Theis, J. A. Cutro, and S. D. Broson, *J. Appl. Phys.* **56**, 401 (1984).
- ³¹ K. S. Seol, A. Ieki, Y. Ohki, H. Nishikawa, and M. Tachimori (unpublished).
- ³² H. Imai, K. Arai, H. Imagawa, H. Hosono, and Y. Abe, *Phys. Rev. B* **38**, 12 772 (1988).
- ³³ A. N. Trukhin, L. Skuja, A. G. Boganov, and V. S. Rudenko, *J. Non-Cryst. Solids* **149**, 96 (1992).
- ³⁴ F. J. Fiegl, W. B. Fowler, and K. L. Yip, *Solid State Commun.* **14**, 225 (1974).

Paramagnetic defect centers induced by excimer lasers, γ rays, and mechanical fracturing in amorphous SiO_2

H. Nishikawa¹ and Y. Ohki²

¹ Department of Electrical Engineering, Tokyo Metropolitan University,
1-1 Minami Osawa, Hachioji, Tokyo 192-03, Japan

² Department of Electrical Engineering, Waseda University
3-4-1 Ohkubo, Shinjuku-ku, Tokyo 169, Japan

Keywords: paramagnetic defect centers, amorphous SiO_2 , excimer laser, γ rays, mechanical fracturing, optical absorption, electron spin resonance

Abstracts. In this paper, we review and examine paramagnetic defect centers in amorphous SiO_2 induced by excimer lasers, γ rays, and mechanical fracturing. Correlation between the paramagnetic defect centers and their precursors introduced during manufacture is discussed for the cases of excimer lasers and γ rays. For the case of mechanical fracturing, formation of strained Si-O-Si bonds as well as paramagnetic defects, is examined. Mechanism of laser- or γ -induced paramagnetic defect centers is compared with that of fracture-induced ones.

Introduction

Over the past several decades, numerous efforts have been devoted to understand basic mechanisms involved in defect formation in amorphous SiO_2 (a- SiO_2) [1], which is an important optical and electronic material in modern technological applications. For example, a- SiO_2 has been used as core of optical fibers, uv-grade optics for excimer lasers, and gate oxides for metal-oxide-semiconductor devices. Optical and electronic properties of this material are in part due to the presence of latent defects introduced during manufacture, which, upon charge trapping or radiolysis, can deteriorate the performance of optical [2] and electronic [3] devices. Mechanical damage such as fiber drawing [4] and fracturing [5] can also induce many defects in a- SiO_2 . Therefore, it is of considerable importance to obtain a detailed understanding of the mechanisms and structures of defects induced by various means.

In order to obtain the structural origins of these defects, electron-spin-resonance (ESR) investigations have been extensively carried out on the radiation-induced defects in a- SiO_2 [1]. Although the ESR is limited to the study of paramagnetic defects, a recent advance in the vuv light sources such as synchrotron radiation allows more detailed study of diamagnetic defects as well as paramagnetic ones by means of optical absorption [6-11] and photoluminescence [12,13] measurements in the uv-vuv regions.

The purpose of this paper is to review some of our efforts to understand the basic mechanisms involved in the defect formations induced by lasers [11,14-17], ionizing radiations [4,18] and mechanical fracturing [19]. Laser-induced defects in silica have been first reported using sub-band-gap photons from excimer lasers [20]. Since then, motivated by technological applications such as optics for excimer-laser lithography in the fabrication process of large-scale-integrated circuits, many

researches have been directed to the defect formation mechanisms. Since diamagnetic defects are typically introduced during manufacturing process of α -SiO₂, they can serve as potential precursors for the paramagnetic defects. Therefore, a principal thrust of this paper is the characterization of the diamagnetic defects and their conversion mechanisms into paramagnetic defect centers. We attempt to explain their formation mechanisms on the basis of the location of the energy levels in the band gap of α -SiO₂. Finally, mechanical fracturing, another means to create paramagnetic defect centers will be discussed in comparison with laser- and radiation-induced defects. Formation of strained bonds by the mechanical fracturing is also discussed based on observation of the increased radiation sensitivity.

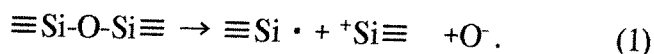
Experimental procedures

Samples used in the present study are high-purity silica prepared by the chemical vapor deposition (CVD) soot remelting, CVD plasma, and flame hydrolysis methods. Ultraviolet (uv) and vacuum uv (vuv) absorption spectra were measured using a conventional visible-uv spectrophotometer (Shimadzu UV-160) and using a synchrotron radiation (SR) facility (0.38 GeV SR ring, Institute for Solid State Physics, the University of Tokyo), respectively. Electron-spin-resonance measurements were carried out at 77 K and at X band frequency using JEOL RE-2XG spectrometer. Fracturing was carried out either by vibrating ball mill or by agate mortar and pestle. Fracturing, shifting, and the sealing of the powdered samples into ESR tubes were done in N₂ gas atmosphere.

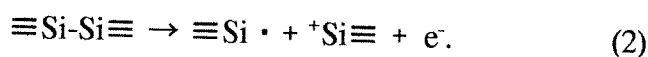
Review of the formation reactions of paramagnetic defect centers

First of all, we will briefly review proposed mechanisms of paramagnetic defect centers.

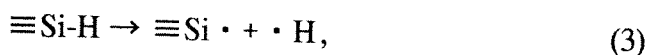
E' center. The E' centers, one of the best known defects in silica glasses, can be induced either by the nonradiative decay of self-trapped exciton wherein an oxygen atom is displaced out of the normal network [21,22]:



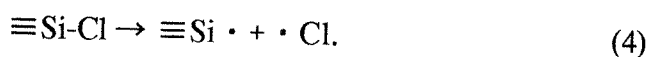
or by the hole trapping at the site of preexisting oxygen vacancy [23]:



Hydrogen and chlorine are the most common impurities in synthetic silica produced by plasma oxidation or hydrolysis of SiCl₄. The Si-H and Si-Cl bonds, probable forms of these impurities, are also regarded as the precursors of the E' centers according to the following reactions [14,15,24,25]:

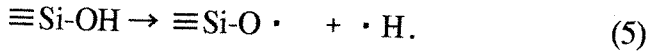


and

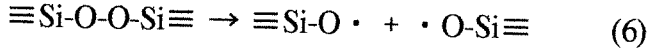


Oxygen hole centers (OHC's). As previously called "wet OHC", nonbridging oxygen hole center (NBOHC) is considered to be induced from hydroxyl incorporated during manufacturing

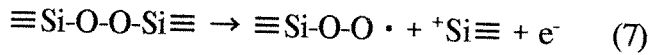
process [26]:



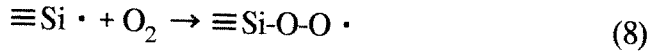
Also in a low-OH oxygen-surplus silica, the NBOHC is proposed to be created from a peroxy linkage [14]:



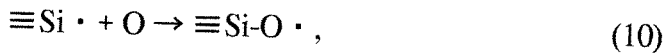
Peroxy radical (PR), previously called "dry OHC", can be observed in low-OH oxygen-surplus silica. It is thought that the PR can be formed by hole trapping on a peroxy linkage [27]:



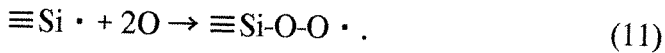
or by the reaction of interstitial molecular oxygen with an E' center [28]:



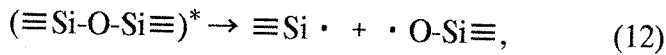
While the reaction of Eq.(8) is a diffusion-limited reaction which can be thermally activated above 200 °C, atomic oxygen induced as a result of photo-induced dissociation ($h\nu > 5.1$ eV) of molecular oxygen can easily diffuse at room temperature and react with an E' center to form NBOHC [15,29] and PR [15]:



and



E'-NBOHC pair creation. Another class of precursor, a strained Si-O-Si bond, can be a precursor for E'-NBOHC pair creation in densified silica [30], mechanically stressed silica [19], and undensified fluorine-doped silica [31]:



where the asterisk indicates a strained state in which bond length or angle is deviated from the normal configuration.

Laser and Radiation Induced Paramagnetic Defect Centers

Precursors introduced during manufacture. As already mentioned, diamagnetic defects introduced in the manufacturing process can act as precursors for the paramagnetic defects when exposed to lasers or ionizing radiations. First, we will see the optical characteristics of these

diamagnetic defects. Ultraviolet-vuv spectra of typical samples are shown in Fig.1. Characteristics of these high-purity silicas are also shown in Table 1. Oxygen-deficient silica (OD2) exhibits an intense absorption band at 7.6 eV, which has been ascribed to oxygen-deficient-type defects [7,8,13]. Oxygen-surplus silica (OS) exhibits a broad absorption tail around 7-8 eV, which has been ascribed to either peroxy linkages [24] or O₂ molecules [29]. While both of these bands due to

nonstoichiometry cannot be seen in the high-OH silica (OH), an absorption tail due to ≡Si-OH bonds [24] is observed as a shoulder beginning at 7.5 eV.

Energy diagram of defect precursors. Possible defect-creation mechanisms are limited by the defect formation energy or the electronic structure of precursor defects. Shown in Fig.2 is the schematic illustration of the energy levels of preexisting defects calculated by O' Reilly and Robertson [32,33]. The valence band (VB) of a-SiO₂ comprises the upper and lower VBs, each corresponding to the oxygen nonbonding and Si-O bonding states, respectively. Energy gaps between the conduction band (CB) and the upper VB and between the CB and the lower VB are shown to be ~9 eV and ~14 eV, respectively.

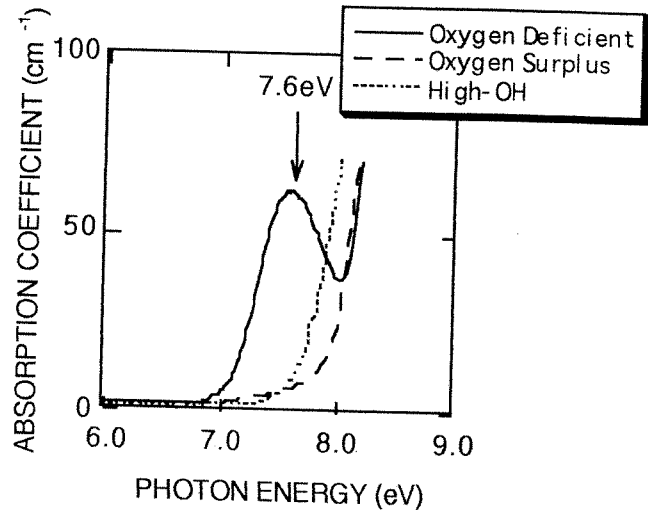


FIG.1 Vacuum ultraviolet absorption spectra of typical types of silicas.

Table 2 shows defect species and their concentration induced by 6.4 eV and 7.9 eV photons, and by ⁶⁰Co γ rays. These data show that defect species are sensitive to the incident-photon energy, as well as to the OH concentration and oxygen stoichiometry.

Figure 3 shows the concentration of defects in oxygen-deficient silica (OD1) induced by 6.4 eV and 7.9 eV lasers as a function of pulse energy. The concentration of the E' centers increases with the square of the laser pulse energy, as shown in the figure, where a log-log plot of the pulse energy versus the defect concentration gives a slope of 2. This indicates that the laser-induced defect formation is

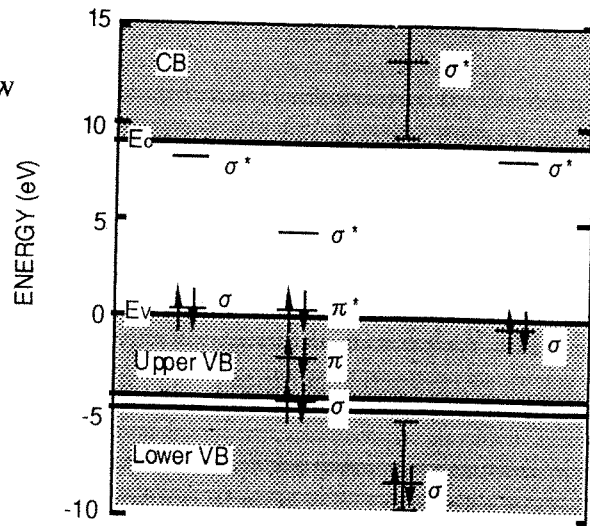


FIG.2 Energy diagram of defects in a-SiO₂

is determined by the two-photon process, which is understood in terms of the cross-band gap excitation of an electron in the VB to CB of a-SiO₂ (E_g ~9 eV) [34].

Photon energy dependence can be understood in terms of the difference in the excitation processes between the cases for two-photon absorption of 6.4 eV or 7.9 eV photons, or for γ-rays. While the

two-photon of 6.4 eV light can only create a hole in the upper VB, the two-photon absorption of 7.9 eV light and γ irradiation can create a hole in the *lower* VB. This means that while the recombination of the electron and hole (e-h) pair created by 6.4 eV excitation gives up energy of ~ 9 eV, recombination of the e-h pair created by 7.9 eV or γ -ray excitation can release an energy of ~ 14 eV.

Now, we examine the defect formation energy of each precursor, one by one. In the present case, we can rule out the case of intrinsic mechanism of Eq.(1) involving the creation of oxygen vacancy and interstitial pair by the nonradiative decay of self-trapped excitons, since it is only possible under "dense excitation" using highly-focused excimer laser [22], which is unattainable in the present experimental conditions.

Then, we will discuss the defect formation from precursors either by the electron rearrangement or by the radiolysis. In the case of the electron rearrangement, the reactions of Eqs.(2) and (7) are induced by the hole trapping at site of the oxygen vacancy and the peroxy linkage, respectively. Since $\equiv\text{Si-Si}\equiv$ has a filled bonding state at ~ 0.5 eV above E_v , the formation of the E' centers through the reaction of Eq.(2) is expected following the hole creation in the *upper* VB. This means that two-photon excitation by 6.4 eV light is sufficient to induce the reaction of Eq.(2). In fact, as shown in Table 2, the E' centers are observed for the cases of both 6.4 eV and 7.9 eV lasers. On the other hand, if we assume that the O-Si bonding state of peroxy linkage lies within the *lower* VB (not reported in the literature), creation of a hole in the *lower* VB is required for the occurrence of the reaction of Eq.(7). That is, at least an energy of 14 eV which is less than the two-photon energy of 7.9 eV light is required. Fig.4 shows the ESR spectra of oxygen-surplus silica exposed to 6.4 eV and 7.9 eV photons. It can be seen that the peroxy radicals (PRs) are only observed for the case of 7.9 eV lasers. Fig.5 shows the change in the vuv spectra of the oxygen-surplus silica OS by 6.4 eV and 7.9 eV lasers. While a notable change is not observed for 6.4 eV laser, a significant decrease of the 7-8 eV band is observed for 7.9 eV laser. The results of Figs.4 and 5 are consistent with the above-mentioned prediction that two-photon excitation by 7.9 eV laser can induce the conversion of the peroxy linkages into the PRs [Eq.(7)]. Gamma-irradiation can also create the PRs, as shown in Table 2.

In the case of the radiolysis, such as Eqs.(3)-(6), the occurrence is determined by the bonding energy $E_{\sigma-\sigma^*}$ [i.e. the energy difference between bonding (σ) and antibonding (σ^*) states] of the respective bonds. If the energy given up by the recombination of e-h pair exceeds the value of $E_{\sigma-\sigma^*}$, the occurrence of the reaction is possible. For example, the value of $E_{\sigma-\sigma^*}$ is estimated to be ~ 8 eV for the Si-H bond and $\sim 15-20$ eV for the O-H bond [35], respectively (see Fig.2). Therefore, while the fission of the Si-H bond is expected by the two-photon absorption of 6.4 eV and 7.9 eV lasers, and by γ -irradiation, that of the O-H bond requires the two-photon absorption of 7.9 eV laser or γ -rays.

We cannot neglect the effect of one-photon process in the case of the precursors exhibiting an optical absorption in the vuv region. For example, the formation of atomic oxygen from interstitial O_2 [Eq.(9)] can be subjected to the photon energy dependence, since the O_2 exhibits an intense absorption (Schumann-Runge band [29]) around 7-8 eV (see Fig.1). In fact, as shown in Fig.4(b), a component of ClO_2 radicals can be only seen in the spectra of oxygen-surplus silica exposed to 7.9 eV photons [15]. The ClO_x radicals can be formed by the reaction of atomic chlorine [from Eq.(4)] with atomic oxygen [from Eq.(9)]:



Therefore, the ESR results shown in Fig.4 indicate that one-photon process is involved for the ClO_x radicals in oxygen-surplus silica OS exposed to 7.9 eV photons. The possible occurrence of these reactions discussed here is summarized in Table 3.

Fracture-Induced Paramagnetic Defect Centers

When mechanical stress is applied to a-SiO₂ by mechanical fracturing, paramagnetic defect centers are induced as in the case of excimer lasers and ionizing radiations. Shown in Table 4 is a result of the fracture-induced paramagnetic defect centers in various types of silica. When compared with the case of lasers and γ rays, one distinctive difference is the fact that both E' centers and NBOHCs are induced by the mechanical fracturing for all samples investigated. Data in Table 4 show that almost a similar number of E' centers and NBOHCs are induced for the relatively stoichiometric sample OH. For the samples with the 5.0 eV absorption band, the E' center is observed in a greater number, whereas for the sample with the 3.8 eV band, the NBOHC is induced in a greater number.

If the normal glass network can be broken, the state directly preceding the bond cleavage, the strained Si-O-Si bond, must have been induced within sample by the mechanical fracturing. In order to check this hypothesis, mechanical fracturing, γ irradiation, and thermal annealing were performed in sequence for the relatively stoichiometric sample OH, as shown in Fig.6. Compared with the case of γ irradiation after the heat treatment, much larger numbers of E' centers and NBOHCs are induced by the γ irradiation immediately after the mechanical fracturing. The schematic of Fig.7 explains these phenomena. Mechanical fracturing creates strained Si-O-Si bonds in the glass network, while at the same time some of the network is broken, forming paramagnetic defect centers. Subsequent γ irradiation results in the formation of paramagnetic defect centers (E' centers and NBOHCs) from these strained bonds. The heat treatment presumably anneals the defect pairs back to normal Si-O-Si bridges, consequently forming stable bonds, which do not serve as precursors for any future paramagnetic defect centers.

Conclusions

We have reviewed our studies on the paramagnetic defect formation in a-SiO₂ by irradiation with excimer lasers, γ -rays, and by mechanical fracturing. In the case of excimer lasers and γ -rays, paramagnetic defect species and their concentrations are strongly influenced by both the manufacturing process and incident-photon energy. The influence of the manufacturing process can be explained by variation in preexisting defect species which can serve as precursors for the paramagnetic defect centers. The defect formation process can be understood in terms of the creation of an e-h pair as a result of two-photon absorption, and subsequent hole trapping or recombination of the e-h pair at the site of the precursors. The photon-energy dependence is explained in terms of the energy levels of the precursor defects in the band gap of a-SiO₂. In the case of mechanical fracturing, the Si-O-Si bond breakage results in the formation E' and NBOHC pairs. In addition to these paramagnetic defect centers, strained Si-O-Si bonds are created, which brings about the enhanced

sensitivity to subsequent γ irradiation.

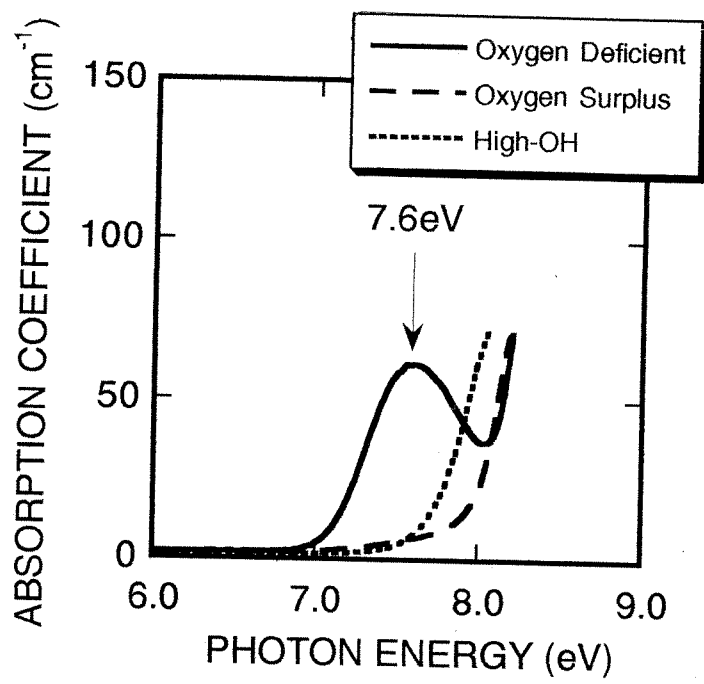
Acknowledgments

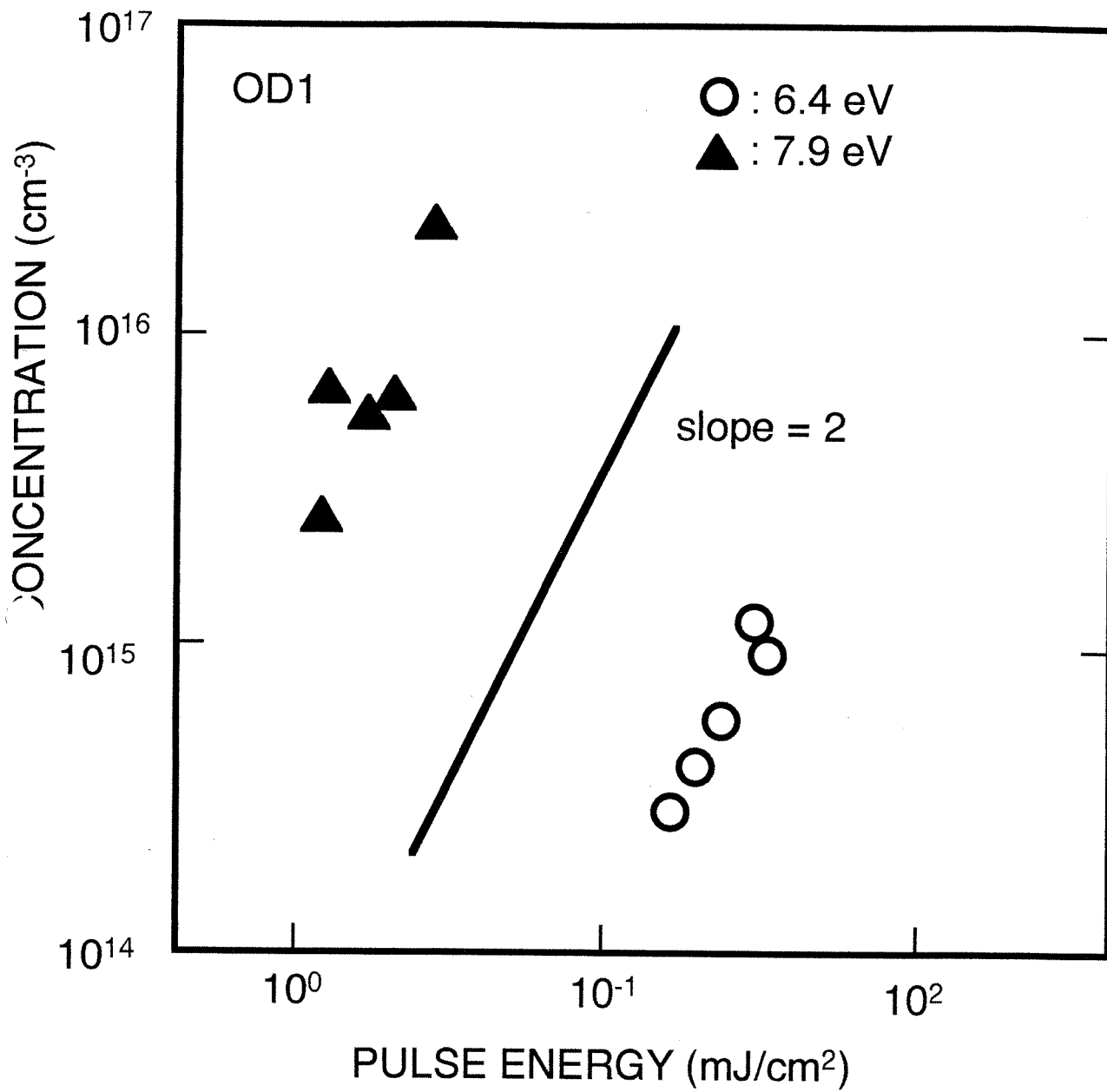
The authors would like to express their thanks to several coworkers, Prof. Y. Hama, Prof. K. Nagasawa, and Dr. R. Tohmon for the useful discussion, and S. Munekuni, R. Nakamura, N. Dohguchi for their help in doing experiments. This work is supported in part by a Grant-in-Aid from the Japanese Ministry of Education, Science, and Culture [No.06452222], by a Grant-in-Aid for Special Research Project from Tokyo Metropolitan University, by the Kanagawa Academy of Science and Technology, by the Casio Science Promotion Foundation and by the Ogasawara Foundation.

References

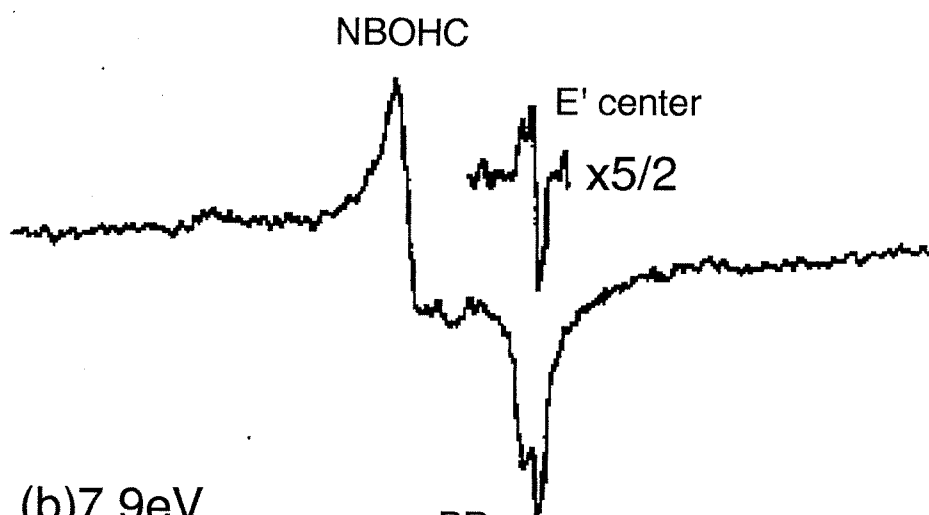
- [1] D.L. Griscom, in *Defects in Glasses*, Vol.61 of Materials Research Society Symposia Proceedings, edited by F.L. Galeener, D.L. Griscom, and M.J. Weber (MRS, Pittsburgh, PA, 1986), p.213.
- [2] D.L. Griscom, *J. Ceram. Soc. Japan*, **99**, 923 (1991).
- [3] W.L. Warren, E.H. Poindexter, M. Offenber, and W. Muller-Warmuth, *J. Electrochem. Soc.* **139**, No.3, 872 (1992).
- [4] K. Nagasawa, Y. Hoshi, and Y. Ohki, *Jpn. J. Appl. Phys. Pt.2*, **26**, L554 (1987).
- [5] K. Kokura, M. Tomozawa, and R.K. MacCrone, *J. Non-Cryst. Solids* **111**, 269 (1989).
- [6] I.P. Kaminow, B.G. Bagley, and C.G. Olson, *Appl. Phys. Lett.* **32**, 98 (1978).
- [7] H. Imai, K. Arai, H. Imagawa, H. Hosono, and Y. Abe, *Phys. Rev. B* **38**, 12772 (1988).
- [8] R. Tohmon, H. Mizuno, Y. Ohki, K. Sasagane, K. Nagasawa, and Y. Hama, *Phys. Rev. B* **39**, 1337 (1989).
- [9] K. Awazu, H. Kawazoe, and K. Muta, *J. Appl. Phys.* **69**, 4183 (1991).
- [10] H. Nishikawa, R. Nakamura, Y. Ohki, and Y. Hama, *Phys. Rev. B* **48**, 15584 (1993).
- [11] R. Tohmon, Y. Shimogaichi, H. Mizuno, Y. Ohki, K. Nagasawa, and Y. Hama, *Phys. Rev. Lett.* **62**, 1388 (1989).
- [12] C.M. Gee and M.A. Kastner, *Phys. Rev. Lett.* **42**, 1765 (1979).
- [13] H. Nishikawa, E. Watanabe, D. Ito, and Y. Ohki, *Phys. Rev. Lett.* **72**, 2101 (1994).
- [14] H. Nishikawa, R. Nakamura, R. Tohmon, Y. Ohki, Y. Sakurai, K. Nagasawa, and Y. Hama, *Phys. Rev. B* **41**, 7828 (1990).
- [15] H. Nishikawa, R. Nakamura, Y. Ohki, K. Nagasawa, and Y. Hama, *Phys. Rev. B* **46**, 8073 (1992).

- [16] H. Nishikawa, R. Nakamura, Y. Ohki, and Y. Hama, Phys. Rev. B **48**, 2968 (1993).
- [17] H. Nishikawa, E. Watanabe, D. Ito, and Y. Ohki, J. Non-Cryst. Solids, **179**, 179 (1994).
- [18] H. Nishikawa, R. Tohmon, Y. Ohki, K. Nagasawa, and Y. Hama, J. Appl. Phys. **65**, 4672 (1989).
- [19] S. Munekuni, N. Dohguchi, H. Nishikawa, Y. Ohki, K. Nagasawa, and Y. Hama, J. Appl. Phys. **70**, 5054 (1991).
- [20] J. H. Stathis and M.A. Kastner, Phys. Rev. B **29**, 7079 (1984).
- [21] T.E. Tsai, D.L. Griscom, E.J. Friebele, Phys. Rev. Lett. **61**, 444 (1988).
- [22] T.E. Tsai and D.L. Griscom, Phys. Rev. Lett. **67**, 2517 (1991).
- [23] F.J. Feigl, W.B. Fowler, and K.L. Yip, Solid State Commun. **14**, 225 (1974).
- [24] H. Imai, K. Arai, H. Hosono, Y. Abe, T. Arai, and H. Imagawa, Phys. Rev. B **44**, 4812 (1991).
- [25] D.L. Griscom and E.J. Friebele, Phys. Rev. B **34**, 7524 (1986).
- [26] M. Stapelbroek, D.L. Griscom, E.J. Friebele, and G.H. Sigel, Jr., J. Non-Cryst. Solids **32**, 313 (1979).
- [27] E.J. Friebele, D.L. Griscom, M. Stapelbroek, and R.A. Weeks, Phys. Rev. Lett. **42**, 1346 (1979).
- [28] A.H. Edwards and W.B. Fowler, Phys. Rev. B **26**, 6649 (1982).
- [29] K. Awazu and H. Kawazoe, J. Appl. Phys. **68**, 3584 (1990).
- [30] R.A.B. Devine and J. Arndt, Phys. Rev. B **42**, 2617 (1990).
- [31] K. Arai, H. Imai, J. Isoya, H. Hosono, Y. Abe, and H. Imagawa, Phys. Rev. B **45**, 10818 (1992).
- [32] E.P. O' Reilly and J. Robertson, Phys. Rev. B **27**, 3780 (1983).
- [33] J. Robertson, in Ref.[1], p.91.
- [34] T.H. Distefano and D.E. Eastman, Solid State Commun. **9**, 2259 (1971).
- [35] When the broad density of states of the Si-OH bonds is taken into account [see Ref.32], the value of the $E_{\sigma-\sigma^*}$ is considered to be distributed from 15 to 20 eV.

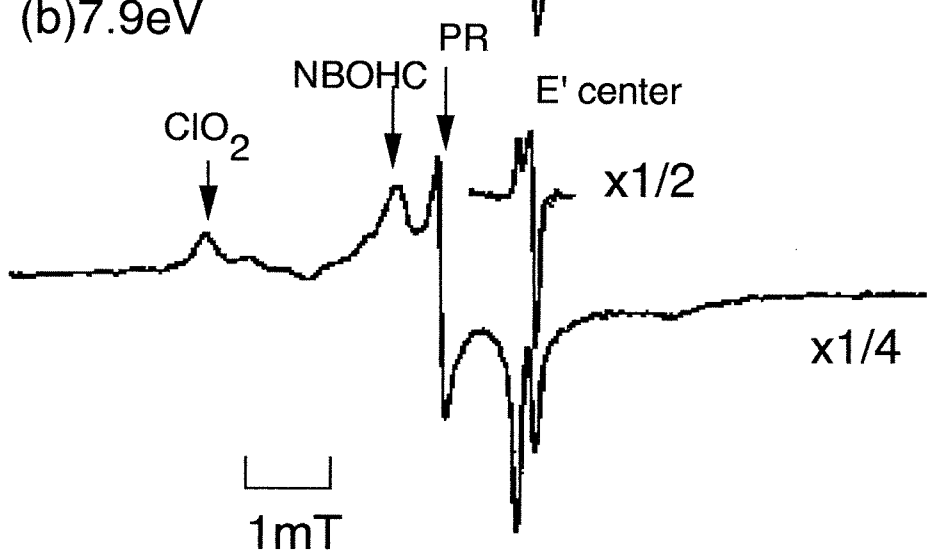


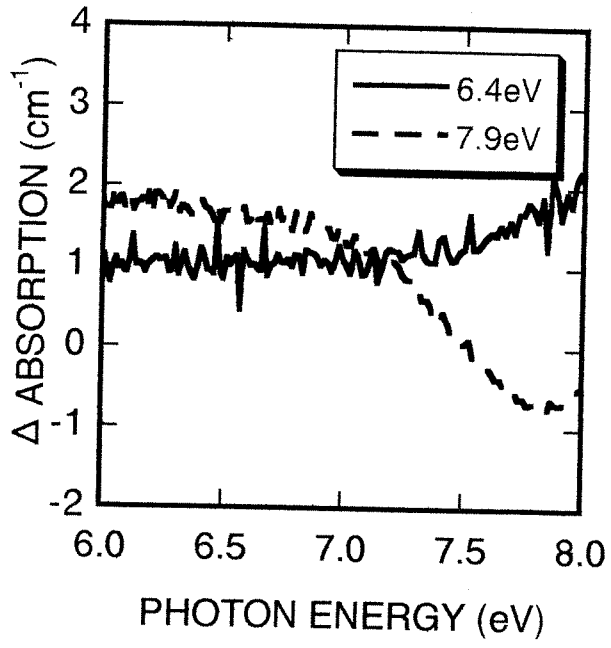


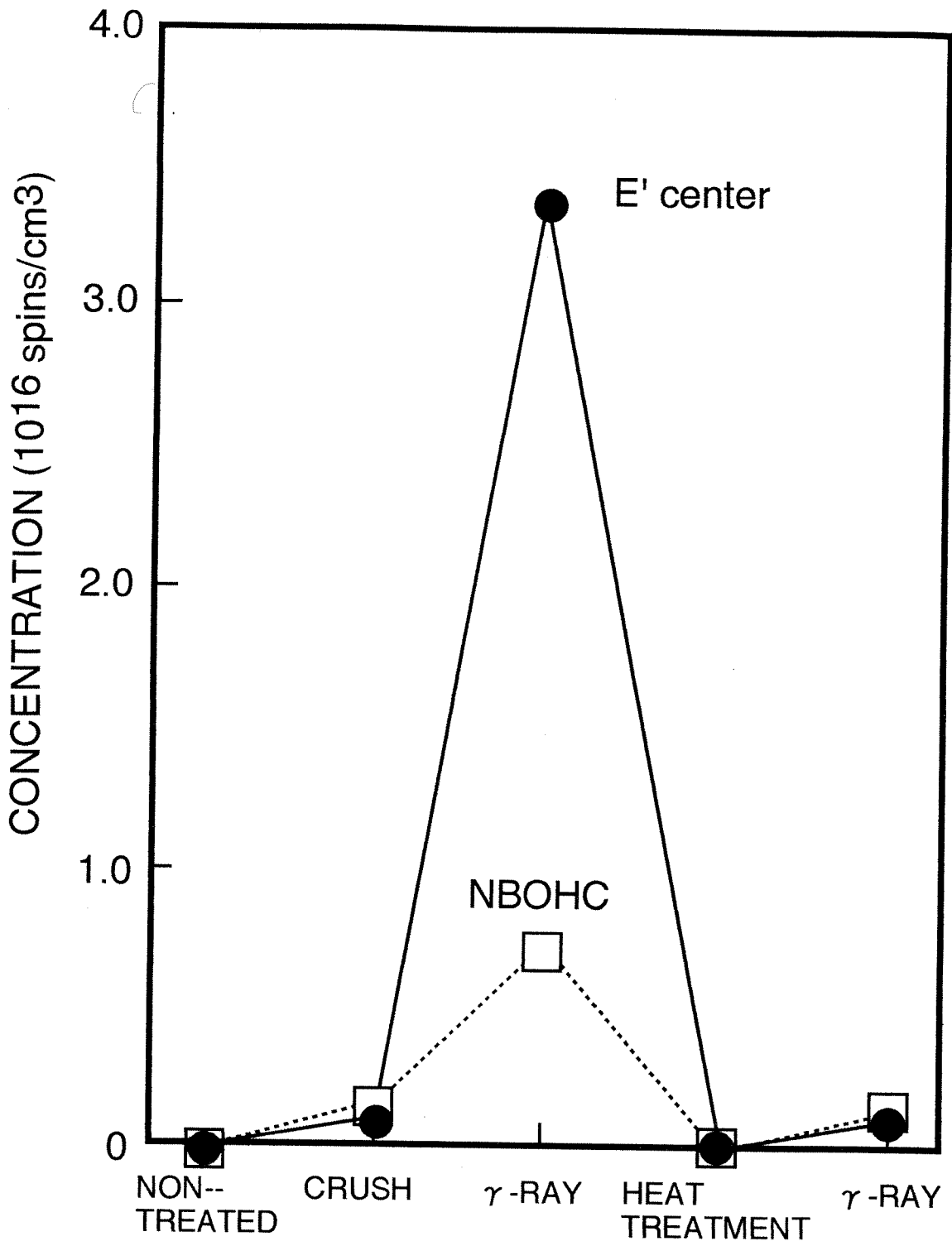
(a) 6.4eV



(b) 7.9eV







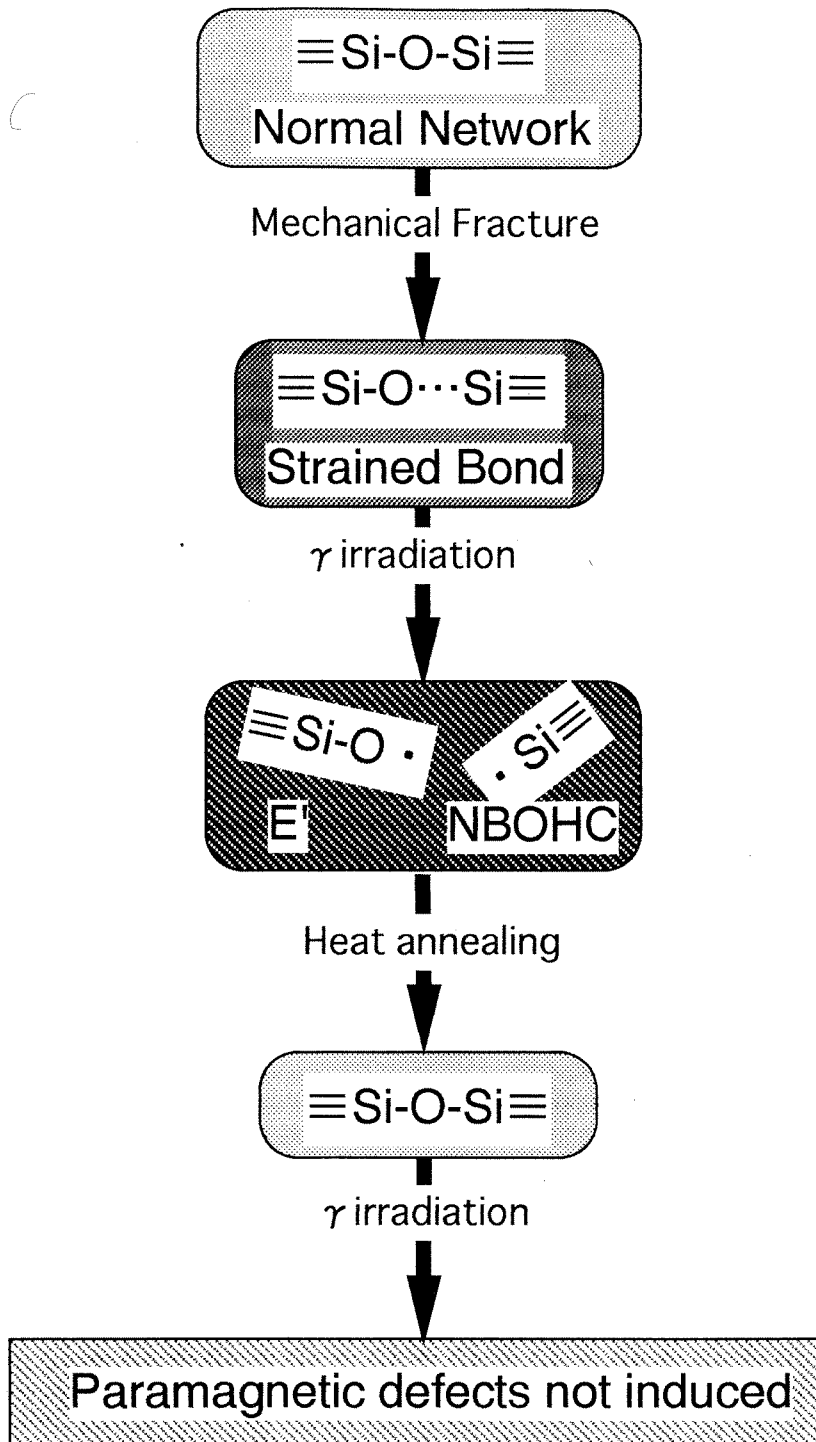


Table 1. Sample list

Sample	Characteristics	Preparation method	Impurities OH [ppm]	Cl [ppm]
OD1	Oxygen deficient	Plasma CVD	0.75	3200
OD2	Oxygen deficient	CVD soot remelting	ND	0.3
OS	Oxygen surplus	Plasma CVD	0.46	370
OH	High-OH (stoichiometric ^a)	Flame hydrolysis	1000	ND ^b

a: No optical absorption bands associated with oxygen vacancy or peroxy linkage [18].

b: ND, not detected.

Table 2. Defect species and their concentration induced by 6.4 eV photons (fluence: 1.8×10^{13} J/cm²), 7.9 eV photons (fluence: 1.5×10^2 J/cm²), and ⁶⁰Co γ -rays (total absorbed dose: 1.4×10^4 Gy)

Radiation	Concentration [10 ¹⁴ cm ⁻³]								
	OD1			OS			OH		
	E'	NBOHC	PR	E'	NBOHC	PR	E'	NBOHC	PR
6.4 eV	6.8	ND ^a	ND	11	180	ND	5.7	ND	ND
7.9 eV	120	ND	ND	150	D ^b	250	26	350	ND
γ rays	76	ND	ND	27	43	6.1	7.2	20	ND

a: ND, Not detected.

b: D, Detected but it was impossible to determine the absolute concentration due to the interference with strong signals of PR and impurity-related radicals.

Table 3. Paramagnetic defect centers induced by 6.4 eV and 7.9 eV photons and by γ -rays, their precursors, and occurrence.

Paramagnetic defect center	Precursor				Occurrence ^a		
	Sample	Type	Species	Density [cm ⁻³]	6.4 eV	7.9 eV	⁶⁰ Co γ
E' center ($\equiv\text{Si}\cdot$)	OD1	Oxygen Deficient	$\equiv\text{Si-Si}\equiv$	$>10^{18}$ ^b	yes	yes	yes
	OD2	Oxygen Deficient	$\equiv\text{Si-Si}\equiv$	7×10^{17} ^b	yes	yes	yes
	OS	Oxygen Surplus	$\equiv\text{Si-Cl}$	7×10^{18} ^c	yes	yes	yes
	OH	High-OH	$\equiv\text{Si-H?}$		yes	yes	yes
NBOHC ($\equiv\text{Si-O}\cdot$)	OS	Oxygen Surplus	$\equiv\text{Si-O-O-Si}\equiv$	7×10^{17} ^d	yes	yes	yes
			$\equiv\text{O}_2\rightarrow 2\text{O}$	$\sim 10^{17}$ ^e	no	yes	yes
			$\equiv\text{Si}\cdot + \text{O}$				
	OH	High-OH	$\equiv\text{Si-OH}$	8×10^{19} ^f	no	yes	yes
PR ($\equiv\text{Si-O-O}\cdot$)	OS	Oxygen Surplus	$\equiv\text{Si-O-O-Si}\equiv$	7×10^{17} ^d	no	yes	yes
			$\text{O}_2\rightarrow 2\text{O}$ $\equiv\text{Si}\cdot + 2\text{O}$	$\sim 10^{17}$ ^e	no	yes	yes

a: Possibility of the reaction occurrence on the basis of the energy diagram (see text and Fig.2)

b: Estimated using absorption cross section of 8×10^{-17} cm² for $\equiv\text{Si-Si}\equiv$ (Ref.[7])

c: Estimated by assuming that all chlorine exists in the form of $\equiv\text{Si-Cl}$

d: Ref.[18]

e: Ref.[29]

f: Estimated from IR absorption at 3650cm^{-1} .

Table 4. Fracture-induced paramagnetic centers and uv absorption in as-manufactured samples.

Sample	Manufacturing method	Type	Cl [ppm]	OH [ppm]	E' center [10 ¹³ spins/cm ³]	NBOHC [10 ¹³ spins/cm ³]	Absorption (as manufactured) [eV]
OH	Flame hydrolysis	High-OH (stoichiometric)	free	1000	53	55	None
OS	Ar+O ₂ plasma	Oxygen Surplus	370	0.46	58	75	3.8
OD3	Ar plasma	Oxygen Deficient	12000	free	95	6.3	5.0
OD4	Ar plasma	Oxygen Deficient	400	3.3	69	13	5.0
OD5	O ₂ plasma	Oxygen Deficient	340	free	140	11	5.0
OD6	CVD soot remelting	Oxygen Deficient	free	free	64	8.8	5.0

Luminescence Properties of Defects in P⁺- or B⁺-implanted Thermally Grown Silicon Dioxide

K. S. Seol, A. Ieki, and Y. Ohki

Department of Electrical Engineering, Waseda University
3-4-1 Ohkubo, Shinjuku-ku, Tokyo 169, Japan

H. Nishikawa

Department of Electrical Engineering, Tokyo Metropolitan University
1-1 Minami-Osawa, Hachioji, Tokyo 192-03, Japan

M. Takiyama

Electronics Research Laboratories, Technical Development Bureau
Nippon Steel Corporation, 5-10-1 Fuchinobe, Sagamihara, Kanagawa 229, Japan

Introduction

Recently, with the scale reduction of very-large-scale-integrated (VLSI) circuits, the quality of gate oxide, which determines such electric properties as breakdown voltage, has become a serious problem. In this situation, defects included in gate oxide are considered to be the most important factor affecting the electric properties of the oxide. Inevitable processes, which induce damages in the gate oxide, exist during the fabrication of metal-oxide-semiconductor (MOS) devices. The ion-implantation process through the gate oxide is one representative of such examples [1]. Since degradation of electrical properties is caused mainly by defects, a study on the defects induced by implantation is very important [2]. However, as for the characterization of the defects existing in thin silicon dioxide (SiO₂) film, a sufficient method has not been established to elucidate the nature of the defects existing in the film. The electron-spin-resonance (ESR), which has been commonly applied to the characterization of SiO₂, is only applicable to paramagnetic defects such as E' center (O₃≡Si ·). However, for diamagnetic and ESR-inactive species such as the oxygen vacancy (O₃≡Si-Si≡O₃), there has not been a good characterization method, although photoluminescence (PL) and optical absorption have been proved to be powerful methods for bulk silica glasses. In this paper, we report PL spectra from P⁺- or B⁺-implanted thermally grown SiO₂ film obtained by synchrotron radiation and excimer laser, and discuss the nature of the defects induced by the ion implantation.

Experimental Procedures

The SiO₂ films used in this study were thermally grown in dry oxygen at 1000 °C on Czochralski p-type (100) Si, and then P⁺ or B⁺ ions were implanted under various conditions. While B⁺ ions were implanted with an acceleration energy of 30 keV to doses from 10¹³ to 10¹⁶ ions/cm², P⁺ ions were done with acceleration energies from 40 to 80 keV to doses from 10¹⁴ to 10¹⁶ ions/cm².

The PL measurement was carried out under excitation by a KrF excimer laser (wavelength: 248 nm, pulse width: ~20 ns) in the temperature range from 88 K to room temperature. The PL spectrum was observed by a multichannel detector equipped with a water cooling system. When the measurement was carried out at low

temperatures, the sample chamber was evacuated to vacuum to prevent from condensation of impurities on the sample surface. The PL decay kinetics in the μ s range was studied under excitation by the KrF excimer laser, while that in the ns range was studied by a time-correlated single photon counting technique using synchrotron radiation under single-bunch operation utilized at BL7B line of UVSOR (Institute for Molecular Science, Okazaki, Japan).

Results and Discussion

Figure 1 shows typical PL spectra taken at room temperature and 88 K from P⁺-implanted thermally grown thin SiO₂ film with an acceleration energy of 80 keV to a dose of 10¹⁵/cm². Three PL bands are observed at 294 nm (4.3 eV), 465 nm (2.7 eV), and 650 nm (1.9 eV). These three PL bands can be observed in all the samples used in this study. The apparent peak at 590 nm is not a real peak but the halftone of the PL peak at 294 nm, since this peak disappeared by cutting photons with wavelengths shorter than 390 nm. The PL bands at 294 nm and 650 nm increase their intensities as the measurement temperature decreases, while the band at 465 nm decreases.

For each PL peak, the decay profile was measured. Figure 2 shows the decay of the 4.3-eV PL band excited by synchrotron radiation in the P⁺-implanted SiO₂ (80 keV, 10¹⁴/cm²) at 20 K. The decay is deviated from a single exponential function, and can be expressed by following equation:

$$I(t) = I_0 \exp(-at - 2bt^{1/2}) \quad (1)$$

Here, a and b are constants and the above equation is known to hold for the PL decay kinetics, if quenching occurs by energy transfer from the donor (excited radiative center) to the acceptor (quenching center) [3]. Quite a similar decay profile was observed for all the other ion-implanted samples.

Figure 3 shows the decay profiles of the PL band at 2.7 eV measured at room temperature for the samples with different doses. The acceleration energy was 80 keV. For all the samples, the 2.7-eV PL decays exponentially, if the initial rapid decay is discarded, regardless of the ion implantation condition. The decay time becomes smaller with an increase in the dose. It is 6.5 ms for the lowest-dose (10¹⁴/cm²) sample and 5.0 ms for the highest-dose (10¹⁶/cm²) sample. However, the decay time scarcely depends on the acceleration energy (data not shown). Shown in Fig. 4 are the decay profiles of the PL at 1.9 eV, measured at various temperatures from 88 K to 280 K. The 1.9-eV PL shows a single exponential decay with the decay constant of 12 μ s at 88 K. The decay profile begins to deviate from single exponential as the measurement temperature increases. Such a tendency is observed for almost all the ion-implanted samples, regardless of the difference in the implantation condition. However, the highest-dose (10¹⁶/cm²) samples seem to have slightly different spectral shape and decay.

It is well known that the 'oxygen-deficient' silica glasses have two PL bands, which are attributed to the oxygen vacancy, at 2.7 eV and 4.3 eV. The properties of these PL bands, including the temperature dependence of PL intensity and the decay profile [4,5], are very similar to those of the PL bands observed in the present ion-implanted SiO₂ film. Therefore, it is considered that the two PL bands at 2.7 eV and 4.3 eV of

the ion-implanted SiO₂ film have the same origins as those of the oxygen-deficient silica glass. The 4.3-eV PL and the 2.7-eV PL are due to the transition from the excited singlet state to the ground singlet state and from the excited triplet state to the ground singlet state, respectively, at the oxygen vacancies induced by ion implantation. This is consistent with the many reports suggesting that the oxygen vacancies are induced by ion implantation in silica glasses [6]. As for the PL at 1.9 eV in the case of bulk silica glasses, the non-bridging oxygen hole center (NBOHC, O₃≡Si-O ·) is accepted to be responsible. It is natural that the laser photons with an energy of 5.0 eV can excite the 1.9-eV PL since this PL is known to have an excitation band at 4.8 eV in the case of bulk silica. The observed decay time of the 1.9-eV PL in the present study, 12 μs, is well consistent with the reported value for bulk silica glasses [5]. Therefore, it is considered that the 1.9-eV PL is due to NBOHCs, except for the highest-dose samples.

Conclusion

We successfully observed photoluminescence from P⁺- or B⁺-implanted thermally grown silicon dioxide film and studied their decay kinetics. The following results were obtained.

- (1) Under the excitation of KrF excimer laser, three PL bands at 4.3 eV, 2.7 eV, and 1.9 eV are observed. As for the PL bands at 4.3 eV and 1.9 eV, the intensity increases with an decrease in the temperature, while it decreases for the PL at 2.7 eV.
- (2) From the similarities of the temperature dependence and the decay profile between the present ion-implanted SiO₂ film and the well-identified bulk silica glass, the two PL bands at 4.3 eV and 2.7 eV are attributable to the oxygen vacancy (O₃≡Si-Si≡O₃), while the PL at 1.9 eV is from NBOHC (O₃≡Si-O ·).

This work was partly supported by a Grant-in-Aid [06452222] from the Ministry of Education, and the Joint Study Program (1992-95) of the Institute for Molecular Science, UVSOR Facility.

References

- [1] E. H. Poindexter and P. J. Caplan, *J. Vac. Sci. Technol.* A6, 1352 (1988).
- [2] M. Offenbergl, M. Major, R. Meyer, and P. Balk, *J. Vac. Sci. Technol.* A4, 1009 (1986).
- [3] Th. Foster, *Naturwiss.* 33, 166 (1946).
- [4] H. Nishikawa, E. Watanabe, and D. Ito, *Phys. Rev. Lett.* 72, 2101 (1994).
- [5] H. Nishikawa, T. Shiroyama, R. Nakamura, Y. Ohki, K. Nagasawa, and Y. Hama, *Phys. Rev.* B45, 586 (1992).
- [6] For example, H. Hosono and N. Matsunami, *Phys. Rev.* B48, 13469 (1993).

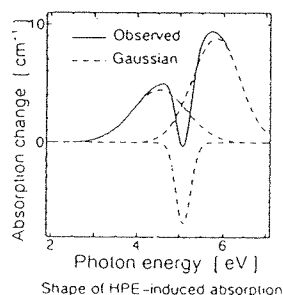
LASER-POWER DEPENDENCE OF KrF EXCIMER LASER INDUCED ABSORPTION IN Ge-DOPED SiO₂ GLASS

Fujimaki, M. Yagi, K. Ohki, Y. *Nishikawa, H. **Awazu, K. ***Muta, K. ***Kato, M. (Waseda University, *Tokyo Metropolitan University, **Electrotechnical Laboratory, ***Showa Electric Wire & Cable Co., LTD)

It is known that structural change is induced in Ge-doped SiO₂ glass when it is irradiated by 5eV photons. Although there have been many reports about this phenomenon (Hosono et al., 1992, Mizrahi & Atkins, 1992, Tsai et al., 1992), the reported structural changes are not consistent. Since Nd:YAG Laser, Hg/Xe lamp and KrF excimer laser were used as the light source in these papers, Tsai et al. inferred the inconsistency is due to the difference of the light power. To elucidate the reason of discrepancy further, we observed the absorption changes induced by KrF excimer lasers.

Sample rods (1cm ϕ \times 10cm) of 1GeO₂:99SiO₂ (mol%) were prepared by the VAD method. The rod was cut into a plate of 0.3mm thick and polished to an optical finish. Two KrF excimer lasers with power of 200 mJ/pulse/cm² (HPE) and 0.5mJ/pulse/cm² (LPE) were used as light sources.

The change induced by HPE is much bigger than that by LPE, when compared at the same irradiated photon numbers. Moreover, the absorption change induced by HPE is bleached by LPE irradiation.



References:

- (1) Hosono et al. (1992) Phys. Rev. B 46 11445
- (2) Mizrahi & Atkins, (1992) Electron Lett. 28(24)2211
- (3) Tsai et al. (1992) Appl. Phys. Lett. 61(4)27

3:45 P.M. **Za3.3**

OPTICAL ABSORPTION AND PHOTOLUMINESCENCE OF DEFECTS IN GERMANIUM-DOPED SILICA GLASSES, M. Fujimaki, Y. Ohki, Waseda Univ., Tokyo; H. Nishikawa, Tokyo Metropolitan Univ., Tokyo; K. Awazu, Electrotechnical Laboratory, Ibaraki; and K. Muta, Showa Electric Wire and Cable Co.Ltd., Kanagawa, JAPAN.

Optical properties of Ge-doped silica glasses were investigated by means of optical absorption and photoluminescence (PL) measurements. Two optical absorption bands at 5.15 eV (241nm) and 6-7 eV, and two PL bands at 3.1 eV (400 nm) and 4.3 eV (290 nm) were observed in the Ge-doped silica. Excitation bands for both PL bands are located at 5.1 eV and 6-7 eV. The decay of the 3.1-eV and 4.3-eV PL bands are exponential with time constants of $\sim 140 \mu s$ and $\sim 9 ns$, respectively. Upon irradiation by a KrF excimer laser (248nm), the decrease in absorption around 5.06eV (245nm) and the increase in absorption around 5.6 eV and 4.4 eV were observed. The origin of these optical absorption and PL bands will be discussed.

Ge ドープ SiO₂ ガラスにおける時間分解励起状態吸収測定

藤巻 真 薛 光洙 大木義路 (早稲田大学)

Time-resolved Excited-state Absorption Measurement in Ge-doped SiO₂ Glass
Makoto Fujimaki, Kwang Soo Seol, and Yoshimichi Ohki (Waseda University)

1. まえがき

Ge ドープ SiO₂ ガラスは、現在、光通信用光ファイバの材料として幅広く用いられ、その普及にはめざましいものがある。そのため Ge ドープ SiO₂ ガラスの光学的特性を調べ理解することは非常に重要である。さらに酸素欠乏型の Ge ドープ SiO₂ ガラスは、光ファイバグレーティングを書き込む材料としても注目を集めている。

これまでに、酸素欠乏型の Ge ドープ SiO₂ ガラスには 5 eV に光吸収帯が観測されており、その吸収帯を励起することにより、4.3 eV (寿命 $\tau < 10\text{ns}$) と 3.1 eV ($\tau = 114 \mu\text{s}$) の発光が生じることが知られている。これらの発光帯は、それぞれ酸素欠乏性欠陥の励起 1 重項 (S_1)、励起 3 重項 (T_1) からの発光であるとされている。¹⁻³⁾ この T_1 状態の緩和時間は、 S_1 状態の緩和時間より遥かに長く、また S_1 から T_1 への緩和時間も 5.3ns と短いため、パワーの強いエキシマレーザで、励起したとき、 T_1 状態にほとんどの電子が上がるということが報告されている。³⁾ また、 T_1 状態に電子が長時間存在していることから、 T_1 からさらに上準位に電子を励起することにより、欠陥のイオン化および構造の変化を、低エネルギーの光子でおこなえる可能性も示唆されている。しかし、 T_1 状態からさらに上準位への励起は、Ge ドープ SiO₂ ガラスでは報告されていない。それゆえ、励起状態からさらに上準位への遷移の測定は、物理学的にも応用面でも非常に重要である。今回我々は、KrF エキシマレーザを励起光源として用い、励起状態からの時間分解光吸収測定を行った。

2. 実験方法

図 1 に測定系を示す。サンプルは、VAD 法により作製した 95SiO₂:5GeO₂ の Ge ドープ SiO₂ ガラスを厚さ 0.3mm 直径 1cm のディスク状に切り研磨して用いた。電子を励起するための光源として使用した KrF エキシマレーザのパワーは 1 パルスあたり、1mJ/cm² でパルス幅は、5ns である。吸収スペクトルを測定するために、白色光源として Xe フラッシュランプをサンプルに照射し、その透過光を分光器に取り込み、マルチチャンネルディテクタによりスペクトルを観測する。なおフラッシュランプとディテクタは、パルスジェネレータにより常に連動しており、露光時間が一定の時には、常に一定の光量がサンプルに入射されるようにする。次に、KrF エキシマレーザを入射し、その時のスペク

トルを同様に観測する。エキシマレーザにより誘起された吸収は、それぞれのスペクトルの差により観測される。またエキシマレーザ照射により発光が生じるが、それは、負の吸収変化として観測される。本実験では、露光時間 30ns で、露光を開始する時間をエキシマレーザ入射後 100ns から 200 μs まで変えて測定を行った。エキシマレーザからの 5eV の強い散乱光がディテクタに入らないように紫外光カットフィルタを使用したため、測定の上限は、4eV (300nm) 程度であり、また、ディテクタの測定限界のため、1.55eV (800nm) 以下は測定できなかった。

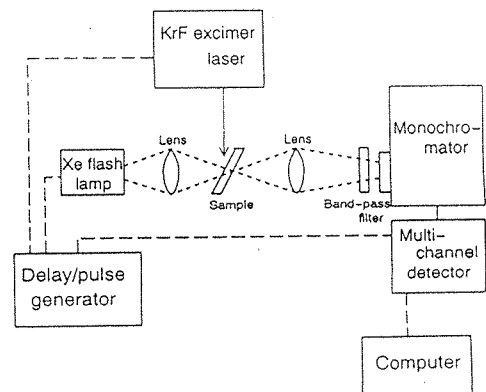


図 1. 時間分解励起状態吸収の測定系
Fig. 1. Time-resolved measurement system for excited-state absorption.

3. 結果と考察

図 2 に測定結果を示す。エキシマレーザ照射により、4eV 付近に過渡吸収が誘起されることが分かる。マイナス方向に生じているピークはエキシマレーザ照射による T_1 状態からの発光である。この図より、エキシマレーザ照射により生じた、4eV 付近の過渡吸収帯は、 T_1 からの発光が減衰していくのと同様の挙動を持って減衰していくことが分かる。つまり、 T_1 状態に電子が存在するときのみこの吸収帯が存在する。このことから、図 2 に見られる吸収帯は T_1 からさらに上準位への電子の遷移であると推測される。

光吸収の立ち上がりをはっきりとさせることを目的として、図 2 のスペクトルからエキシマレーザ照射に

より生じる T_1 状態からの発光を差し引いたものを図 3 に示す。上準位への電子遷移による光吸収は、3eV 付近から立ち上がり、4eV 以上にピークを持つブロードなスペクトルを持つことが分かる。すなわち、基底状態から見て 6 eV から始まり 7 eV 以上にピークを有する幅広い吸収と言うことになる。これまでに Ge ドープ SiO_2 ガラスのバンドギャップは、7.1eV であるとの報告もあり⁴⁾、今回測定された吸収は、おそらく伝導帯による吸収であろうと推測される。いずれにせよ、今回 T_1 状態からの励起が測定できたことは、酸素欠乏性欠陥の光学的特性をさらに理解する上でも、また、 T_1 状態からの励起により、欠陥のイオン化が、基底状態からのイオン化よりも低エネルギーの光子で行えるという可能性の追求においても大きな意味を持つ。

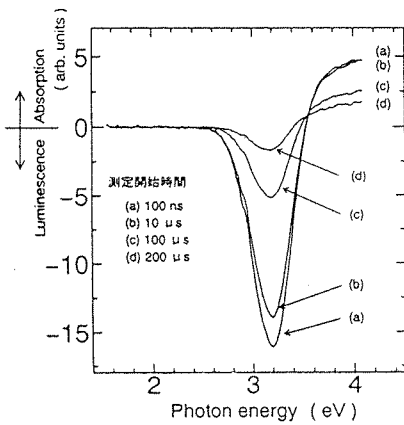


図 2. 時間分解励起状態吸収の測定結果
Fig. 2. Observed results of the time-resolved excited-state absorption measurements.

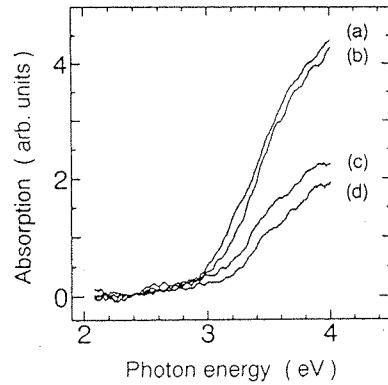


図 3. 励起状態吸収スペクトル
(a)-(d)は図 2 と同じ
Fig. 3. Excited-state absorption spectra.
(a)-(d) are the same as indicated in Fig. 2.

文献

- 1) M. J. Yuen, Appl. Opt. **21**, 136 (1982).
- 2) L. Skuja, J. Non-Cryst. Solids **149**, 77 (1992).
- 3) V. N. Bagratashvili et al., Opt. Lett. **20**, 1619 (1995).
- 4) J. Nishii et al. Opt. Lett. **20**, 1184 (1995).

Ge ドープ SiO₂ ガラスにおける励起状態吸収測定

Excited-state absorption measurement in Ge-doped SiO₂ glass

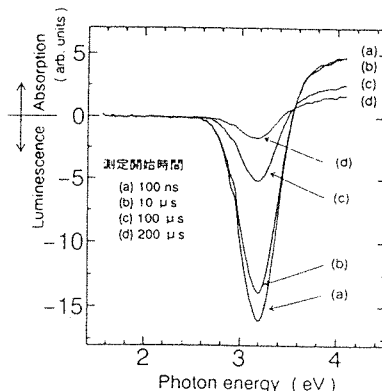
早稲田大学 藤巻 真 薛 光洙 大木義路

Waseda Univ. M. Fujimaki K. S. Seol Y. Ohki

1. まえがき Ge ドープ SiO₂ ガラスは、現在、通信用光ファイバの材料として、幅広く用いられ、さらに、酸素欠乏型の Ge ドープ SiO₂ ガラスは、光ファイバグレーティングを書き込む材料としても注目を集めている。今回我々は、ガラス内の酸素欠乏性欠陥の励起三重項状態からの光吸収の測定に成功したので報告する。

2. 実験方法 サンプルは、VAD 法により作製した Ge 濃度 5 mol% のプリフォームロッドを、厚さ 0.3mm、直径 1cm のディスク状に切り研磨して用いた。電子を励起するための光源としては、KrF エキシマレーザを用いた。吸収スペクトルを測定するために、サンプルに白色光源である Xe フラッシュランプを照射し、その透過光スペクトルをディテクタにより測定する。励起状態吸収は、エキシマレーザ光を照射した時としない時のスペクトルの差により求められる。本実験では、励起状態吸収の時間変化を観測するため、Xe ランプの露光時間を 30ns、露光を開始する時間を、エキシマレーザ入射後、100ns から 200 μs まで変えて、測定を行った。

3. 実験結果 右図に測定結果を示す。4eV 付近に吸収帯が誘起されることが確認された。3.1eV 付近に見られる負のピークは、エキシマレーザ照射によるガラス内の酸素欠乏性欠陥の発光であると考えられる。またこの発光は、酸素欠乏性欠陥の励起三重項状態(T₁)からの発光に帰属されている。観測された吸収帯は、この発光と同一の挙動を持って減衰していくことから、この吸収帯は、T₁ からさらに上準位への電子遷移によるものであると考えられる。



励起状態吸収の測定結果

27a-F-8

Ge ドープ SiO₂ ガラスにおける KrF エキシマレーザ誘起光吸収のフォトリーチ

Photo-bleach of KrF excimer laser induced absorption in Ge-doped SiO₂ glass

・藤巻 真・ 八木幹太・ 大木義路・ 西川宏之^b 粟津浩一^c 牟田健一^d 加藤真基重^d

M. Fujimaki K. Yagi Y. Ohki H. Nishikawa K. Awazu K. Muta M. Kato

a 早稲田大学 b 東京都立大学 c 電総研 d 昭和電線

Waseda Univ. Tokyo Metro. Univ. ETL SWCC

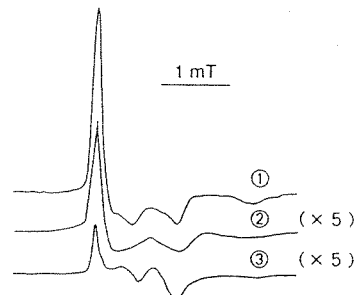
【はじめに】 我々はこれまでに、高い光子密度の KrF エキシマレーザ光 (5 eV) を照射することにより Ge ドープ SiO₂ ガラスに誘起される吸収は、低い光子密度の KrF エキシマレーザ光照射によってブリーチされることを報告した¹⁾。しかし誘起された 4.5 eV 帯と 5.8 eV 帯の 2 つの吸収帯は、いずれも 5 eV に吸収の裾を持っているため、ブリーチ光として KrF エキシマレーザを用いたのでは、どちらの吸収帯が、フォトリーチ過程に関与しているのかわからない。そこで今回、低光子密度の ArF エキシマレーザ (6.4 eV) および Xe ランプを光源に用いフォトリーチを観測した。

【実験方法】 サンプルとして Ge 濃度 5 mol% の VAD プリフォームロッドを厚さ 0.3mm に研磨して用いた。パワー密度約 70 mJ/cm² per pulse の KrF エキシマレーザを 20 shots 照射することにより吸収を誘起した後、パワー密度約 0.3 mJ/cm² per pulse の ArF エキシマレーザ、および Xe ランプを紫外光カットフィルタ (4 eV 以上をカット) を通して照射することによって、吸収のフォトリーチを観測し、同時に ESR スペクトルの測定を行い、ブリーチされていく常磁性欠陥を調べた。

【実験結果】 高光子密度の KrF エキシマレーザ光を試料に照射した後、ESR スペクトルを求めると、見かけ上殆ど GEC に帰属できると思われるスペクトル①が得られた。この試料に低光子密度の ArF エキシマレーザ光を照射しフォトリーチさせると、スペクトルは①と同じ形状のまま強度が減少する (スペクトル②)。これに対して Xe ランプ光によりフォトリーチすると、ESR シグナル強度の減少につれて、E' 中心に帰属できると思われるスペクトル③と変化していった。なお、virgin 試料に同じ時間 Xe ランプのみを照射しても、E' 中心は誘起されなかった。

【参考文献】 1) 藤巻他：第 55 回応用物理学学会学術講演会、21a-K-4

【謝辞】 本研究は一部、文部省科研費一般 (B) の援助を受けた。



- ①、高光子密度の KrF エキシマレーザ照射により誘起された ESR シグナル
- ②、低光子密度の ArF エキシマレーザ照射によりフォトリーチを行った時の ESR シグナル
- ③、Xe ランプ照射によりフォトリーチを行ったときの ESR シグナル

28p-ZE-2

Ge ドープ SiO₂ ガラスのエキシマレーザ光多量照射による光吸収変化

Absorption change in Ge-doped SiO₂ glass induced by irradiation of a large number of excimer laser photons

八木幹太^a 藤巻 真^a 大木義路^a 西川宏之^b 粟津浩一^c 牟田健一^d 加藤真基重^d

K. Yagi M. Fujimaki Y. Ohki H. Nishikawa K. Awazu K. Muta M. Kato

a 早稲田大学 b 東京都立大学 c 電総研 d 昭和電線

Waseda U. T. M. U. ETL SWCC

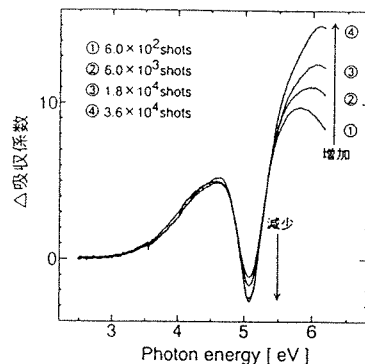
【はじめに】 我々は、これまでに Ge ドープ SiO₂ ガラスに KrF エキシマレーザ (5.0eV) を照射すると、5.0eV 付近の吸収が減少し、4.5eV と 5.8eV 付近の吸収がほぼ 1 対 1 の割合で増加する事を観測した¹⁾。しかしながら、さらにエキシマレーザ光の照射を続けていったときには、誘起される吸収の変化が異なることを見出したので報告する。

【実験方法】 サンプルとして Ge 濃度 1 mol% の VAD プリフォームロッドを厚さ 0.3mm に研磨して用いた。パワー密度約 100 mJ/pulse の KrF エキシマレーザを 10Hz で照射し、誘起される吸収の変化を測定した。

【実験結果】 右図に示すように、4.5eV、5.8eV 付近の吸収の増加がほぼ飽和した後、エキシマレーザをさらに照射 (~3.6 × 10⁴ shots) していくと、5.0eV 付近の吸収が引き続いて減少するとともに高エネルギー側に新たな吸収の増加が生じることが観測された。4.5eV、5.8eV 付近の吸収は大気中 450°C での熱アニールにより 10 分程度でほぼ消滅するのに対して、新たに生成された高エネルギー側の吸収は消滅しにくい。

本研究は一部、文部省科研費一般研究 B【No. 06452222】の援助を受けて行われた。

【参考文献】 1) 藤巻他：第 55 回応用物理学学会学術講演会、21a-k-4



エキシマレーザ光子 (5eV, 100mJ/pulse) を多量に照射した時の吸収変化

21a-K-4

GeドープSiO₂ガラスにおけるKrFエキシマレーザー誘起光吸収のレーザーパワー依存性
Laser-power dependence of KrF excimer laser induced absorption in Ge-doped SiO₂ glass

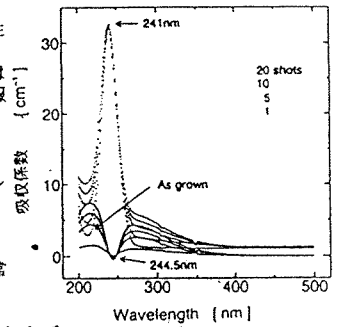
藤巻 真 八木幹太* 大木義路* 西川宏之* 栗津浩一* 牟田健一* 加藤真基重*
M. Fujimaki K. Yagi Y. Ohki H. Nishikawa K. Awazu K. Muta M. Kato
a 早稲田大学 b 東京都立大学 c 電総研 d 昭和電線
Waseda U. T. M. U. ETL STCC

【はじめに】 GeドープSiO₂ガラスに5eVの光を照射すると、ガラス内部に構造の変化が誘起され、光吸収に変化が生じる。このことについては、すでに様々な報告がなされている¹⁻⁴⁾。5eVの光源として、YAG:Ndレーザーの倍波、Hgランプ、KrFエキシマレーザー等、様々なものが用いられているが、報告されている誘起変化は必ずしも一定ではない。この原因を調査するため、パワーの異なるエキシマレーザーを用いて、誘起される吸収変化の違いを調べたので報告する。

【実験方法】 サンプルとしてGe濃度1mol%のVADプリフォームロッドを厚さ0.3mmに研磨して用いた。パワー密度約40mJ/cm²・shotと約0.01mJ/cm²・shotのKrFエキシマレーザーを照射し、吸収の変化を測定した。またパワー密度約40mJ/cm²・shotのKrFエキシマレーザーを数十shots照射したのち、パワー密度約0.01mJ/cm²・shotのKrFエキシマレーザーを照射し、その時の吸収の変化を測定した。

【実験結果】 右図に示すように、パワー密度約40mJ/cm²・shotのレーザーを照射すると、244.5nmにピークを持つ吸収帯が減少していき、220nm付近と280nm付近の吸収が増加していくことがわかる。パワー密度約0.01mJ/cm²・shotのレーザーを照射したときも、同様の変化がみられるが、このときの吸収の変化は、照射フォトン数が同数でも、前者のものより非常に小さい。さらにパワー密度約40mJ/cm²・shotのレーザーを照射した時に生じた吸収の変化は、パワー密度の小さいレーザーを照射していくにつれて回復していくことがわかった。

【参考文献】 1)H. Hosono et al. Phys. Rev. B 46 11445(1992) 本研究は一部科研費一般(B) [06452222]および
2)Y. Mizrahi et al. Electron. Lett. 28(24) 2211(1992) コーニングリサーチグラントの援助を受けた。
3)T. E. Tsai et al. Appl. Phys. Lett. 61(4) 27(1992)



パワー密度約40mJ/cm²・shotのエキシマレーザー照射による吸収の変化
— はレーザーを照射したときの吸収の変化

21a-K-5

GeドープSiO₂ガラスの発光の励起帯の温度依存性
Temperature dependence of the excitation spectra of the luminescence of Ge-doped SiO₂ glass

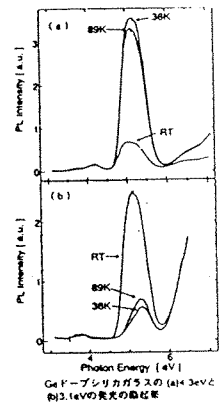
藤巻 真 八木幹太* 大木義路* 西川宏之* 栗津浩一* 牟田健一* 加藤真基重*
M. Fujimaki K. Yagi Y. Ohki H. Nishikawa K. Awazu K. Muta M. Kato
a 早稲田大学 b 東京都立大学 c 電総研 d 昭和電線
Waseda U. T. M. U. ETL STCC

【はじめに】 近年、GeドープSiO₂ガラスにおける発光や光吸収の特性について、様々な報告がなされているが、そのメカニズムにはいまだに解明されていない点が多い。これらの特性の解明は、この素材の光デバイスへの応用に際して、非常に重要である。今回この発光の励起帯の温度依存性を測定したので報告する。

【実験方法】 サンプルとして、Ge濃度1mol%のVADプリフォームロッドを厚さ0.3mmに研磨して用いた。励起光としては、岡崎分子科学研究所のUVSORからのSR光をSeya-Namioka型分光器にて分光し、励起光を紫外から真空紫外の範囲で掃引し、4.3eV(290nm)と3.1eV(400nm)の二つの発光帯をモニターした。またサンプルを常温から39Kまで冷却し、励起帯の温度依存性を測定した。

【実験結果】 図(a)(b)は、それぞれ4.3eV、3.1eVでモニターした励起スペクトルである。またRT、89K、38Kは、それぞれ測定温度を示す。5eVと真空紫外域より裾を引く2つの励起帯が観測された。4.3eV発光の励起帯は、5eVのピーク、真空紫外域の裾の両者とも低温になるにつれて、その強度が小さくなっている。一方、3.1eV発光の励起帯は、5eV付近のピークは、低温において常温よりも小さく、真空紫外域の裾は、温度にあまり影響されないことがわかる。

本研究は一部科研費一般(B) [06452222]およびコーニングリサーチグラントの援助を受けた。



Geドープシリカガラスの(a)4.3eV、(b)3.1eVの発光の励起帯

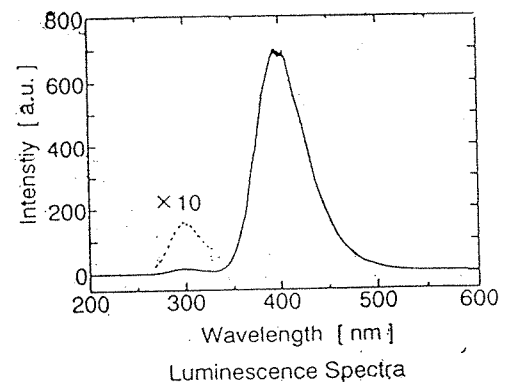
27p-L-2

Geドープシリカガラスのエキシマレーザー誘起ルミネッセンス
Excimer laser induced luminescence in Ge-doped silica glass

早稲田大学 東京都立大* 藤巻真 西川宏之* 大木義路
Waseda Univ. Tokyo Metropolitan Univ.* M. Fujimaki H. Nishikawa* Y. Ohki

近年Geドープのシリカガラスによる非線形効果、例えば第2次高調波発生(SHG)や光誘起屈折率変化などが報告されている。これらの現象はレーザー光により誘起される欠陥が主な原因と考えられている。一方、ガラス中の欠陥はレーザー光照射によるルミネッセンスを発するものが多く、欠陥構造の研究においてレーザー誘起ルミネッセンスは有力な手がかりを与える。そこで、今回GeドープシリカガラスにArFエキシマレーザー(λ=193nm)を照射し発光を観測した。

YAD法で合成した、OH濃度 約50ppm、Cl濃度 約300ppm、Ge濃度 約8~13mol%を含むシリカガラスを用意し、ArFエキシマレーザーによる発光測定(大気中、室温)を行ったところ、右図に示す様に400nmと290nm付近に発光のピークが見られた。



Luminescence Spectra